

KfK 3378  
Februar 1983

# Optical Potentials and Isoscalar Transition Rates from 104 MeV Alpha-Particle Scattering by the N = 28 Isotones $^{48}\text{Ca}$ , $^{50}\text{Ti}$ and $^{52}\text{Cr}$

R. Pesl, H. J. Gils, H. Rebel, E. Friedman, J. Buschmann,  
H. Klewe-Nebenius, S. Zagromski  
Institut für Angewandte Kernphysik  
Institut für Radiochemie

**Kernforschungszentrum Karlsruhe**



KERNFORSCHUNGSZENTRUM KARLSRUHE

Institut für Angewandte Kernphysik  
Institut für Radiochemie

KfK 3378

OPTICAL POTENTIALS AND ISOSCALAR TRANSITION RATES  
FROM 104 MeV ALPHA-PARTICLE SCATTERING  
BY THE N=28 ISOTONES  $^{48}\text{Ca}$ ,  $^{50}\text{Ti}$  AND  $^{52}\text{Cr}$

R. Pesl, H.J. Gils, H. Rebel, E. Friedman<sup>+</sup>,  
J. Buschmann, H. Klewe-Nebenius and S. Zagromski

Kernforschungszentrum Karlsruhe GmbH, Karlsruhe

---

<sup>+</sup>Racah Institute of Physics, The Hebrew University, Jerusalem, Israel

Als Manuskript vervielfältigt  
Für diesen Bericht behalten wir uns alle Rechte vor

Kernforschungszentrum Karlsruhe GmbH  
ISSN 0303-4003

## ABSTRACT

Precisely measured differential cross sections for elastic and inelastic scattering from 104 MeV alpha-particles by  $^{48}\text{Ca}$ ,  $^{50}\text{Ti}$  and  $^{52}\text{Cr}$  are reported. The analyses aim primarily at the determination of strength, radial shapes and deformation of the scattering potentials, looking for isotonic differences of N=28 isotones. The mean square radii of the (real) potentials are discussed in terms of mean square radius differences of the matter distributions. The isoscalar transition rates derived by coupled channel analyses of the measured cross sections are compared with electromagnetic rates. In addition to the analyses on the basis of a slightly generalized extended optical model a semi-microscopic deformed folding model has been applied, using a density-dependent effective alpha-bound nucleon interaction. Though an excellent description of the data over the full angular range is obtained the resulting values of the deformation parameters appear to be not consistent with results from various different methods.

OPTISCHE POTENTIALE UND ISOSKALARE ÜBERGANGSRATEN AUS DER STREUUNG VON 104 MeV ALPHA-TEILCHEN AN DEN N=28 ISOTONEN  $^{48}\text{Ca}$ ,  $^{50}\text{Ti}$  und  $^{52}\text{Cr}$

## ZUSAMMENFASSUNG

Es wird über genaue Messungen der differentiellen Wirkungsquerschnitte für die elastische und unelastische Streuung von 104 MeV Alpha-Teilchen an  $^{48}\text{Ca}$ ,  $^{50}\text{Ti}$  und  $^{52}\text{Cr}$  berichtet. Die Analysen zielen in erster Linie auf eine Bestimmung der Stärke, radialen Gestalt und Deformation der optischen Potentiale ab, wobei auf isotonische Differenzen in der N=28 Reihe geachtet wird. Die mittleren quadratischen Radien der (reellen) Potentiale werden im Hinblick auf Radiusdifferenzen der Materieverteilung der Kerne diskutiert. Mit Hilfe der Methode der gekoppelten Kanäle und einer "Radial momentum analysis" der Potentiale werden aus den gemessenen Wirkungsquerschnitten isoskalare Übergangsraten gewonnen und mit elektromagnetischen Raten verglichen. Neben den Analysen auf der Basis eines makroskopisch deformierten optischen Potentials (bei leichter Verallgemeinerung

der Standard-Form) wird ein halb-mikroskopisches deformiertes Faltungsmodell angewandt, das eine dichteabhängige effektive Wechselwirkung zwischen Alpha-Teilchen und gebundenen Kernnukleonen benutzt. Obwohl eine bemerkenswert gute Beschreibung der Daten über den vollen Wechselbereich erreicht wird, sind die Werte für die Deformationsparameter nicht konsistent mit Resultaten, die unabhängig mit anderen Methoden gewonnen werden.

## 1. INTRODUCTION

The nuclei of the Ca region provide a unique testing ground for investigating interesting nuclear structure effects associated with adding valence nucleons to closed-shell cores<sup>1</sup>. Electron scattering<sup>2</sup>, muonic X-ray studies<sup>3,4</sup> and high-resolution laserspectroscopy<sup>5,6</sup> have established a very peculiar variation of the nuclear charge radii of the Ca isotopes, increasing in the first half of the  $1f_{7/2}$  neutron shell and decreasing in the second half. In contrast, hadron scattering<sup>7-9</sup> probing the *matter* and *neutron* distributions reveals an approximately monotonic increase of the matter radii between  $^{40}\text{Ca}$  and  $^{48}\text{Ca}$ . In the isotonic chain of  $^{48}\text{Ca}$ - $^{50}\text{Ti}$ - $^{52}\text{Cr}$  the roles of protons and neutrons appear to be changed, and when increasing the charge the  $f_{7/2}$  valence protons may induce similar polarization effects to the  $N=28$  neutron core as the  $f_{7/2}$  neutrons do for the  $Z=20$  proton distributions of Ca isotopes. In fact, the polarization of the proton core of  $N=28$  isotones has been already demonstrated<sup>4</sup> by high-accuracy measurements of charge distribution differences, and there remains the interesting question how the neutrons respond to the addition of valence protons.

Studies of matter- and neutron distributions inevitably rely on strongly interacting probes, and this implies additional uncertainties in interpreting the experimental results. Nevertheless, there seems to be increasing consistency of recent results of various approaches using different hadronic probes, in particular, of high energy proton scattering and medium energy alpha-particle scattering<sup>9</sup>. The increased confidence in using alpha-particle scattering as a tool for exploring nuclear matter distributions is borne out by precisely measured cross sections, by refined and reliable methods of analyses<sup>10</sup> and by an improved understanding<sup>11,2</sup> of the alpha-particle - nucleus interaction in terms of the nuclear density distributions (involved in the scattering process). The required information is accessible mainly from the real part of the interaction potential which is well described by the first order expression (folding model) of the multiple scattering

expansion of the optical potential, thus reflecting in a simple and rather direct way size and shape of the underlying matter distributions. Therewith, alpha-particle scattering in the energy range of 100 MeV does not only probe the nuclear surface, but proves to be additionally sensitive to the nuclear interior, so that the ms radii of the distributions appear to be well defined by the experiment<sup>12</sup>.

In this paper we report the results of precision measurements of elastic and inelastic scattering of 104 MeV alpha-particles from  $^{48}\text{Ca}$ ,  $^{50}\text{Ti}$  and  $^{52}\text{Cr}$ . The measured differential cross sections extend over a wide angular range, including the "nuclear rainbow" region<sup>13</sup> where alpha-particle scattering exhibits refractive properties of the optical potential and hence some transparency of the interior of the probed nucleus. The analyses of the experimental data aim primarily at the determination of strength, radial shapes and deformation of the scattering potentials, which provide a good basis of a well-founded discussion of nuclear density distributions. Some global aspects of the optical potentials derived from the data have been already discussed in context of studies<sup>12</sup> of the energy and mass number dependence of the alpha-particle-nucleus potential. The studies presented here emphasize the isotopic differences and their relevance to the nuclear structure of N=28 isotones. Since changes in the ms deformation of the nuclei will affect isotopic and isotonic radius differences<sup>14</sup>, the analysis of inelastic scattering may provide valuable information about a possible correlation of this kind. In our case, we have to consider the deformation of the matter distributions as derived from isoscalar transition rates which are not necessarily equal to corresponding electromagnetic transition probabilities. Recently an improved method<sup>15</sup> for extracting reliable values of isoscalar transition rates from  $(\alpha, \alpha')$  data has been proposed and demonstrated just by application to the  $^{50}\text{Ti}(\alpha, \alpha')$  and  $^{52}\text{Cr}(\alpha, \alpha') 0^+ \rightarrow 2_1^+$  differential cross sections, so that part of the necessary information is already available. In the present paper, we study the (presumably dynamic) quadrupole deformation of  $^{50}\text{Ti}$  and  $^{52}\text{Cr}$  additionally by a somewhat more



direct, but model-dependent approach, based on a description<sup>16</sup> of the deformed real potential by folding a deformed density distribution with an explicitly specified effective  $\alpha$ -bound nucleon interaction.

## 2. EXPERIMENTS

The measurements of the differential cross sections of the elastic and inelastic scattering from ground and low-lying excited states used the 104 MeV alpha-particle beam and the scattering facilities of the Karlsruhe Isochronous Cyclotron. The extracted alpha-particle beam was passed through a  $150^\circ$  analyzing magnet and focussed on target with a beam spot of approximately 1.5 mm in diameter with the aid of several quadrupole doublets. The energy spread of the beam was reduced to 50-100 keV. The targets were uniform, self-supporting metal foils, isotopically highly enriched and ranging from 1 to 7 mg/cm<sup>2</sup> in thickness. The scattered alpha-particles were detected by seven Si surface barrier detectors of 4 mm active thickness and mounted on two movable arms inside a 130 cm  $\emptyset$  scattering chamber. Using 1.5 mm slits in front of the detectors an angular resolution of the complete experimental set up of less than  $0.2^\circ$  was achieved. The conventional electronic set up consisted of standard NIM modules and data acquisition system based on a NOVA II computer. The resulting overall energy resolution of 150-180 keV (FWHM) was sufficient to separate elastic, inelastic and contaminant (C,0) peaks at almost all scattering angles. Particle identification was not necessary because the maximum energy loss of other possible reaction products (p,d,t,<sup>3</sup>He) in the detectors used are outside of the interesting energy region of the spectra (for <sup>3</sup>He due to distinctly different Q-values). Checks of the absolute zero point of the angular scale were done by measuring the elastic scattering cross section for <sup>40</sup>Ca and by comparing with results precisely measured previously<sup>8</sup>. The total uncertainty of the absolute values of the scattering angles is about  $\pm 0.05^\circ$ . At each scattering angle the spectra of alpha particles scattered

from each of the targets were measured in turn in order to avoid angular error by new settings. The experiments cover an angular range from  $\theta_{CM} = 2.5^\circ$  to  $100^\circ$ . The diffraction region was measured in angular steps of  $0.5^\circ$ , the region beyond  $\theta_{CM} \geq 60^\circ$  in steps of  $1.5^\circ$ . A well-shielded Faraday cup behind the scattering chamber controlled the beam current. The accumulated charge was typically between 10 and 2500  $\mu\text{Cb}$  providing sufficient statistical accuracy also for excitation of the weakly excited  $4_1$  states. Since by purely experimental considerations (target thickness, integrated beam current, detector acceptance) the absolute scale of the cross sections can be determined only within 10 % accuracy, the data have been finally normalized at forward angles to reliable optical model predictions<sup>16</sup>.

Figs. 1 and 2 display the experimental differential cross sections measured with  $^{50}\text{Ti}$  and  $^{52}\text{Cr}$  targets. The data for  $^{48}\text{Ca}$  (elastic scattering alone, shown in Fig. 3) are essentially identical with the results of ref. 8, slightly improved in accuracy in the nuclear rainbow region. The error bars include uncertainties of the absolute scattering angle, converted into a cross section errors. Some more details of the experimental procedures and tabulated values of the cross sections are given elsewhere<sup>17</sup>.

### 3. OPTICAL MODEL ANALYSIS OF ELASTIC SCATTERING

Analyses of elastic scattering of alpha particles have shown that the radial shape of the real part of the optical potential is significantly better approximated by a squared Saxon-Woods form ( $\text{SW}^2$ ) rather than by the standard Saxon-Woods (SW) parametrization<sup>18</sup>

$$U(r_\alpha) = -V_O f_V(r_\alpha) - i W_O f_W(r_\alpha) + V_C(r_\alpha) \quad (3.1)$$

with

$$f_{V,W}(r_\alpha) = \{1 + \exp((r_\alpha - R_{V,W})/a_{V,W})\}^{-1} \quad (3.2)$$

and  $V_C$  the Coulomb-potential of realistic charge distributions.

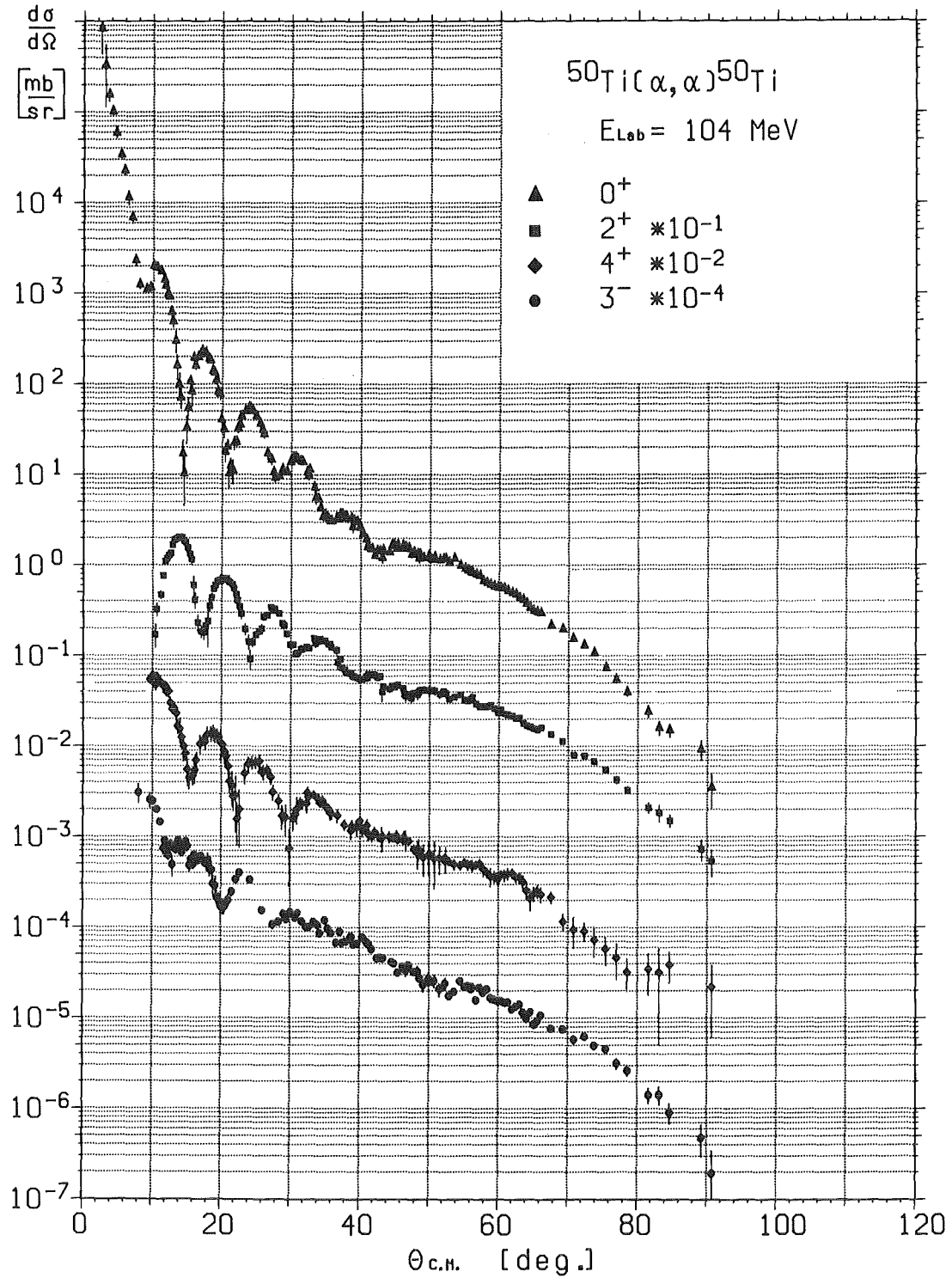


Fig. 1 Experimental cross sections of elastic and inelastic scattering of 104 MeV alpha particles from  $^{50}\text{Ti}$

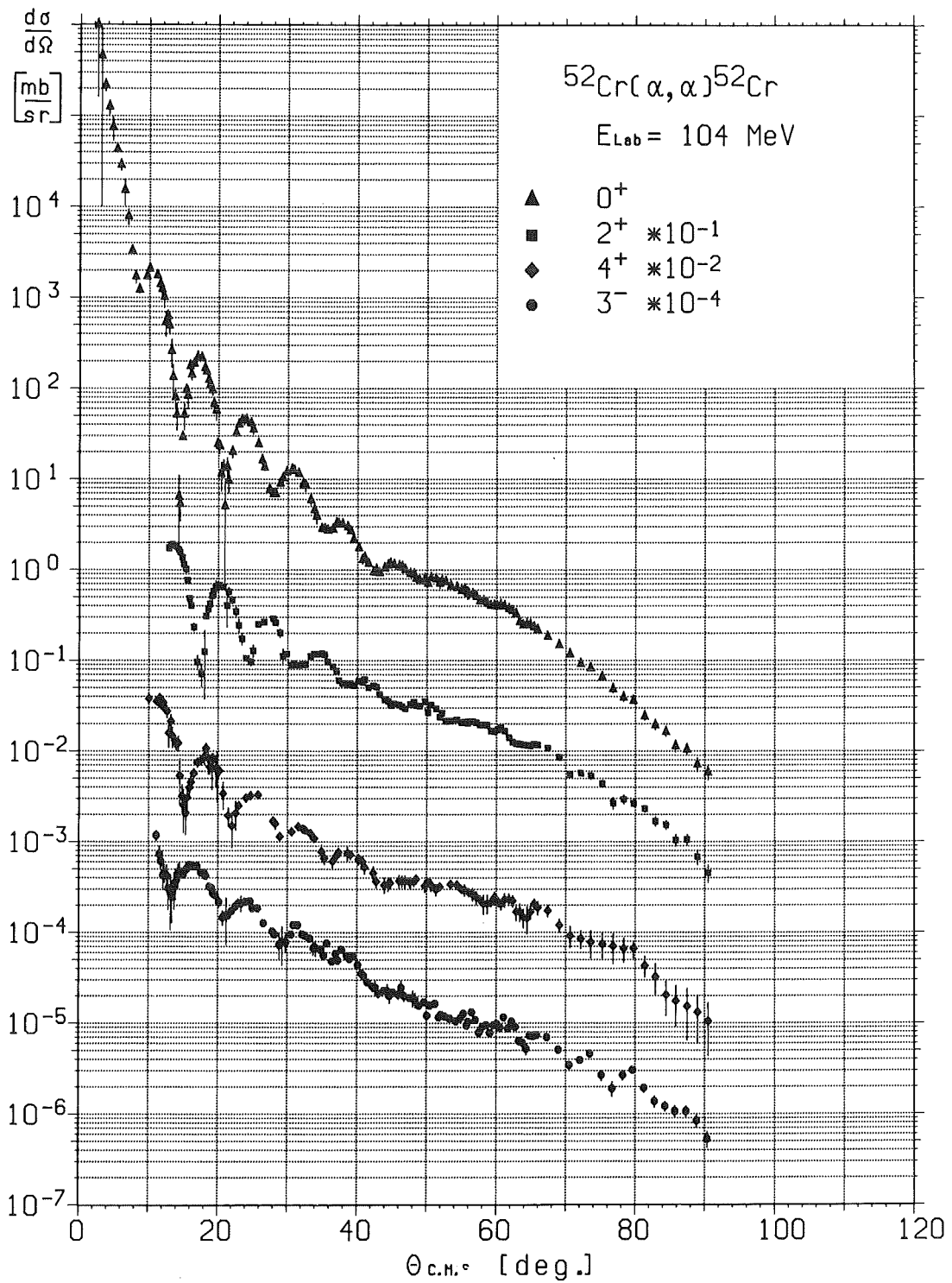


Fig. 2 Experimental cross sections of elastic and inelastic scattering of 104 MeV alpha particles from  $^{52}\text{Cr}$

This is again confirmed by our data<sup>17</sup> as demonstrated in Fig. 3. Table 1 gives the best fit parameters obtained with a  $(SW)^2$  parametrization of the real part of the optical potential.

Introducing the  $SW^2$  form also in the imaginary part of the optical potential the  $\chi^2$  values are only slightly reduced, and the improvement in describing the data seems not to be significant.

In studies of isotopic and isotonic effects the choice of particular simple functional forms for the potentials may introduce some constraints. In order to reduce such effects we apply one of the recent flexible methods<sup>10,12</sup>, model-independent in the sense that they allow more general and less monotonic radial shapes. The real part of the optical potential was therefore written as

$$U_R(r_\alpha) = -V_B(r) - \sum_{n=1}^N b_n j_0\left(\frac{n\pi r}{R_C}\right) \quad (3.3)$$

where  $V_B(r)$  is the fixed  $SW^2$  best-fit potential. In the range  $r < R_C$ , where  $R_C$  is a suitable chosen cut-off radius (usually 9-13 fm) the shape of  $V_B$  is corrected by a series of spherical Bessel functions. The  $N$  coefficient  $b_n$  ( $N=10-13$ ) were adjusted by fitting the experimental data. In order to reduce the (weak) dependence of the results on the chosen values of  $R_C$  and  $N$ , the fits have been repeated with several combinations ( $N, R_C$ ), and the results were finally averaged. In addition to its flexibility, the Fourier-Bessel method provides realistic errors of the potential distributions (shown as "error bands" in Fig. 5 and 6). The resulting theoretical differential cross sections are displayed in Fig. 4, and the values of integral quantities are given in Table 2. All optical model calculations of elastic scattering cross sections used the computer code MODINA<sup>19</sup>.

Table 1 Best fit parameters and integral quantities of real  $SW^2$  and imaginary SW potentials

A	$V_0$ [MeV]	$r_V$ [fm]	$a_V$ [fm]	$-J_V/4A$ [MeV fm <sup>3</sup> ]	$\langle r_V^2 \rangle^{1/2}$ [fm]	$W_0$ [MeV]	$r_W$ [fm]	$a_W$ [fm]	$-J_W/4A$ [MeV fm <sup>3</sup> ]	$\langle r_W^2 \rangle^{1/2}$ [fm]	$\chi^2/F$
<sup>48</sup> Ca	162.1	1.38	1.27	318.6	4.46	28.9	1.63	0.60	95.0	5.11	3.3
<sup>50</sup> Ti	147.1	1.41	1.20	307.5	4.47	20.1	1.60	0.58	94.6	5.05	1.8
<sup>52</sup> Cr	157.1	1.31	1.23	300.6	4.45	22.5	1.53	0.67	97.0	5.09	1.7

Table 2 Integral quantities of FB potentials

	$-J_V/4A$ [MeV fm <sup>3</sup> ]	$\langle r_V^2 \rangle^{1/2}$ [fm]	$-J_W/4A$ [MeV fm <sup>3</sup> ]	$\langle r_W^2 \rangle^{1/2}$ [fm]	$\chi^2/F$
<sup>48</sup> Ca	325 ± 4	4.51 ± 0.03	96.0	5.09	2.3
<sup>50</sup> Ti	304 ± 4	4.45 ± 0.025	93.0	5.09	1.5
<sup>52</sup> Cr	300 ± 4	4.46 ± 0.025	96.0	5.08	1.5

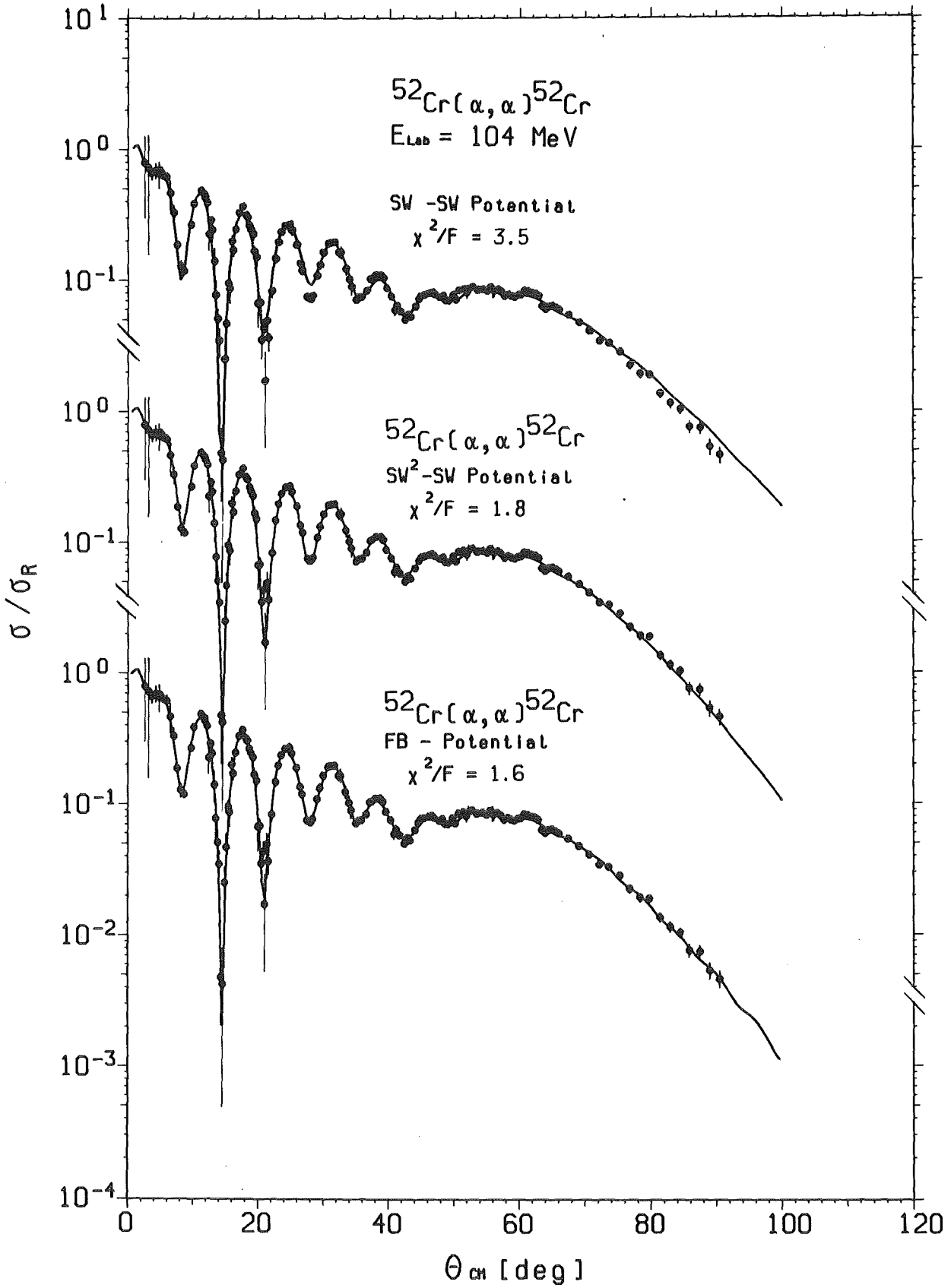


Fig. 3 Phenomenological optical model descriptions of elastic 104 MeV alpha-particle scattering from  $^{52}\text{Cr}$  with different radial shapes of the real potential

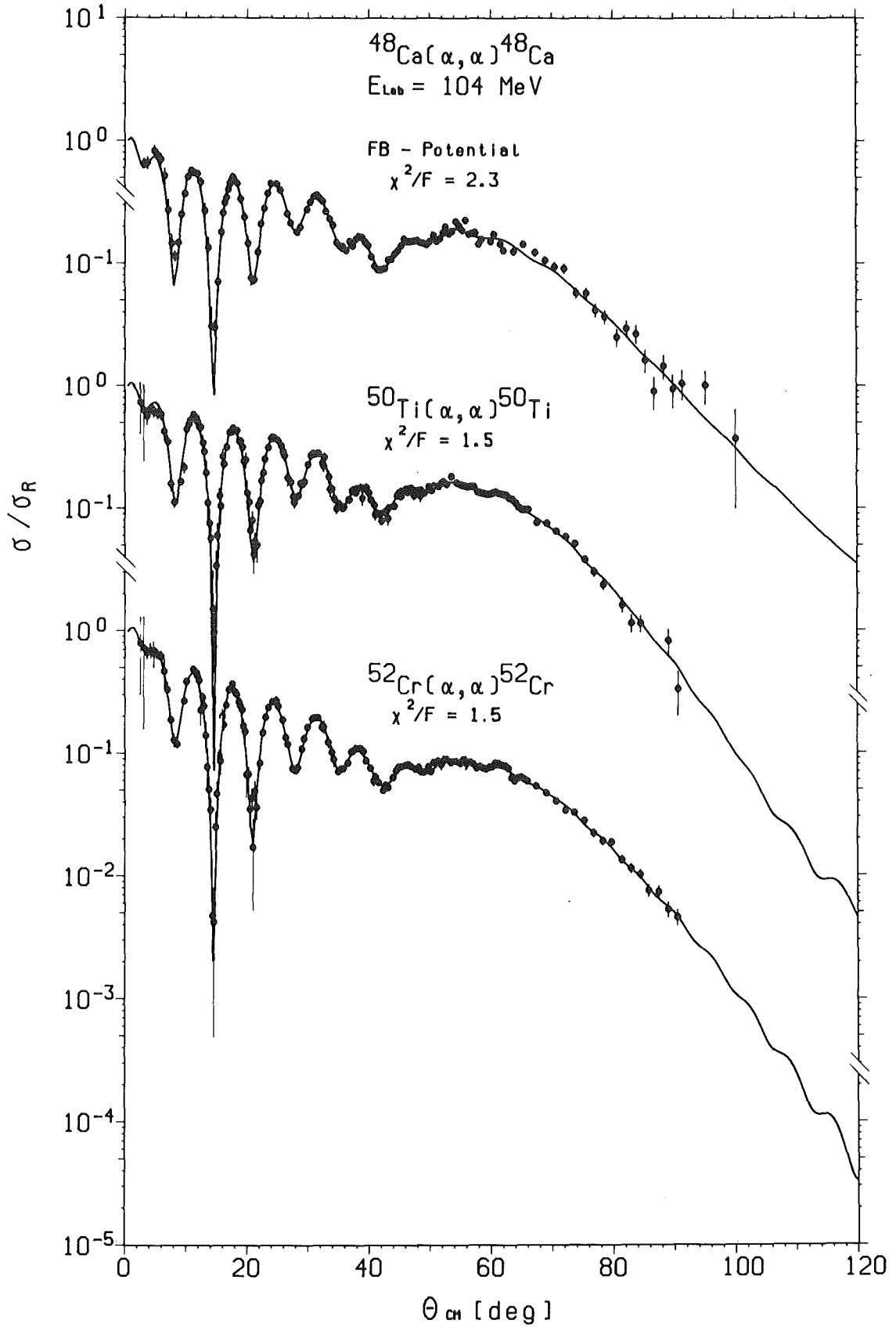


Fig. 4 Elastic scattering of 104 MeV alpha-particles:  
Results of the Fourier-Bessel analysis.



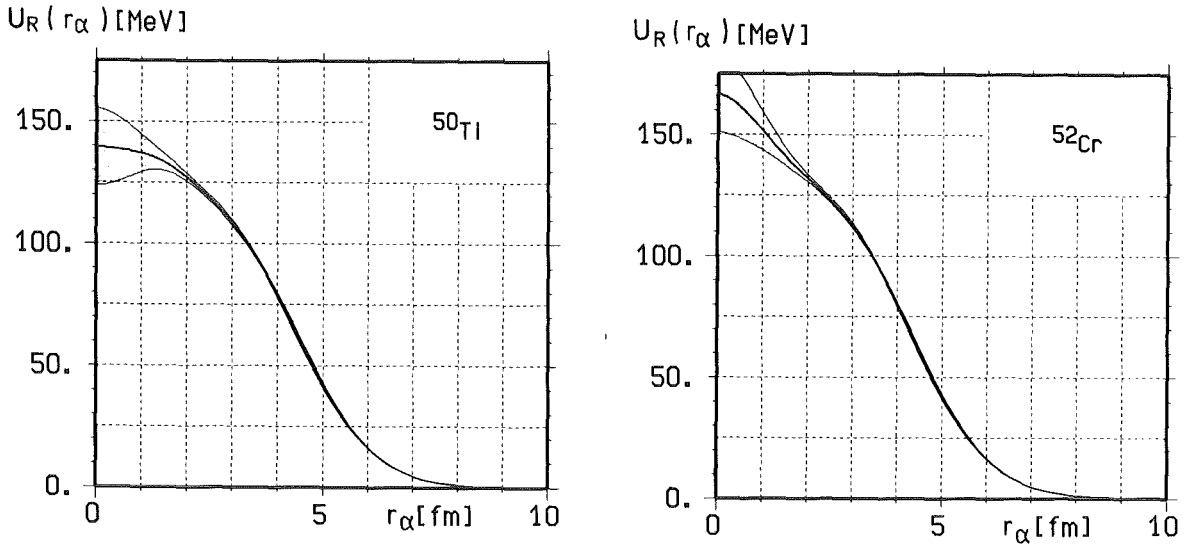


Fig. 5 Real Fourier-Bessel potentials obtained by 104 MeV alpha-particle scattering

#### 4. NUCLEAR MATTER RADII

The precise information obtained on the optical potentials describing the elastic scattering can be used also to extract some parameters related to the density distribution of nuclear matter in the nuclei involved. Studies<sup>12</sup> of the dependence on energy and on mass-number of integral quantities of the real part of the optical potentials (such as the volume integral and rms radius) strongly indicate that a folding model description of the potential is a very good approximation. In this model the real part of the optical potential is related to the nuclear density distribution via an effective  $\alpha$ -nucleon interaction,

$$U_R(r_\alpha) = \int V_{\alpha N} (|\vec{r}-\vec{r}_\alpha|) \rho_m(\vec{r}) d^3r \quad (4.1)$$

Although it was shown<sup>8</sup> that in explicit folding model fits to elastic scattering data one must introduce fairly large saturation effects into the  $\alpha$ -N interaction, the above mentioned studies<sup>12</sup> show that these density-dependent effects are rather similar in different nuclei. As a consequence it is possible to make a folding model interpretation of the real part of the optical

potential, and in particular, to apply the additivity of mean square radii to the extraction of rms radii of nuclear density distribution, namely

$$\langle r_v^2 \rangle = \langle r_m^2 \rangle + \langle r_{\text{eff}}^2 \rangle \quad (4.2)$$

where  $\langle r_{\text{eff}}^2 \rangle$  is the m.s. radius of the effective interaction obtained from a similar interpretation of the optical potential for a nucleus whose density distribution is assumed known. For the present analysis we use  $\langle r_{\text{eff}}^2 \rangle = 7.8 \pm .25 \text{ fm}^2$  obtained<sup>8</sup> from a similar analysis of the elastic scattering of 104 MeV  $\alpha$  particles by  $^{40}\text{Ca}$ . It should, however, be emphasized that such a folding model interpretation is probably reliable only for nuclei not too far apart in the periodic table.

Table 3 Various nuclear rms radii for the N=28 isotones

target	$\langle r_{\text{ch}}^2 \rangle^{1/2}$ [fm]	$\langle r_{\text{p}}^2 \rangle^{1/2}$ [fm]	$\langle r_{\text{m}}^2 \rangle^{1/2}$ [fm]	$\delta \langle r_{\text{m}}^2 \rangle^{1/2}$ [fm]
$^{48}\text{Ca}$	3.481 $\pm$ .005	3.40	3.54 $\pm$ .051	-
$^{50}\text{Ti}$	3.57 $\pm$ .005	3.50	3.46 $\pm$ .046	-.08 $\pm$ .046
$^{52}\text{Cr}$	3.65 $\pm$ .030	3.57	3.48 $\pm$ .048	-.06 $\pm$ .048

Table 3 summarizes the results for the N=28 isotones. In calculating differences  $\delta \langle r_{\text{m}}^2 \rangle^{1/2}$  the uncertainty in  $\langle r_{\text{eff}}^2 \rangle$  was not included because it affects equally both values of  $\langle r_{\text{m}}^2 \rangle^{1/2}$  which are being compared.

From combined analyses of electron scattering and muonic X-ray data<sup>4</sup> we know that the sequential addition of proton pairs to the  $1f_{7/2}$  orbital results in an approximately linear decrease in successive isotonic shifts of charge radii. Taking into account the "trivial" contribution from spatial distribution  $\rho_{\text{p}}$  of the  $1f_{7/2}$  shell protons, the core polarization, represented by

$\Delta\rho_{\text{ch}}^{\text{core}} = \rho_{\text{ch}}^{Z+2} - (\rho_{\text{ch}}^Z + 2\rho_p)$ , has been revealed. The effects induced by neutrons and protons are very similar, with  $\delta\langle r^2 \rangle_{\text{ch}}^{\text{core}}$  values positive in the first half of the  $f_{7/2}$  shell and negative in the second half<sup>4</sup>. It is interesting to note that by adding a proton pair to  $^{48}\text{Ca}$  the rms radius of the nuclear matter distribution first decreases and then remains almost constant.

As far as the differences in the real optical potentials (extracted by the Fourier-Bessel procedure) reflect the shapes of matter distribution differences, Fig. 6 indicates that the main effect is due to the additional  $f_{7/2}$  protons reducing the neutron-proton radius difference existing in  $^{48}\text{Ca}$ . But, in addition, the  $f_{7/2}$  protons may influence the neutron distributions as well.

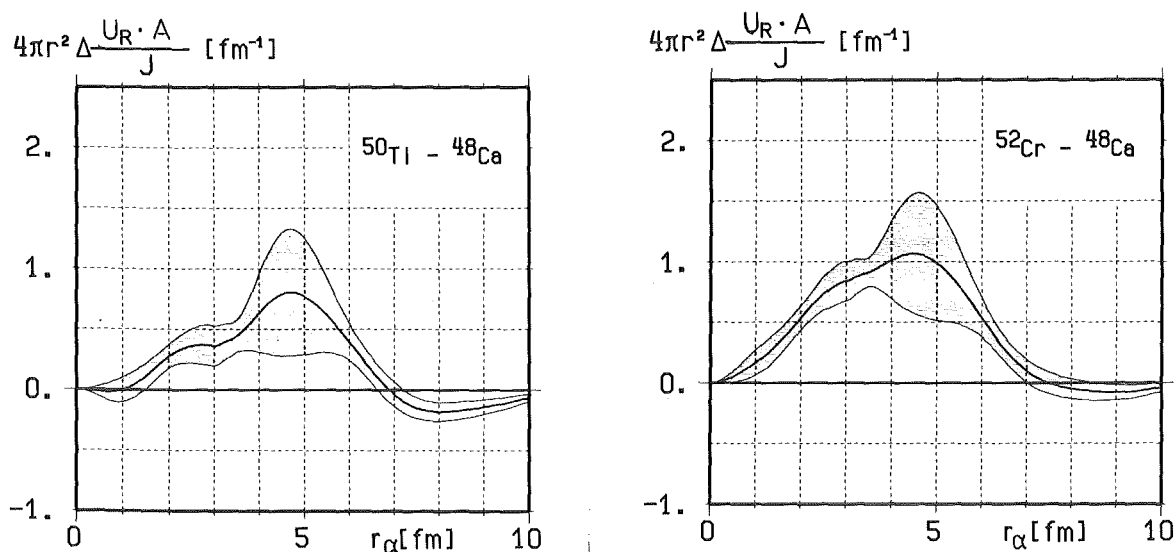


Fig. 6 Differences between real potentials extracted by the Fourier-Bessel analysis of elastic 104 MeV alpha-particle scattering

This information should be available more directly from a detailed folding model analysis<sup>20</sup>, combined with precisely measured charge distribution differences.

## 5. INELASTIC SCATTERING ANALYSES

### 5.1 Extended Optical Model

In the framework of the collective model the non-diagonal part  $U_{\text{coupl}}$  of the complex interaction potential providing the coupling of different nuclear states is deduced from an extended optical potential

$$U(r_\alpha) = -V_0 f(\vec{r}_\alpha) - iW_0 g(\vec{r}_\alpha) \quad (5.1)$$

deformed by the angular dependence of the half-way radius e.g.

$$R(\hat{r}_\alpha) = R_0 \left( 1 + \sum_{\lambda\mu} \alpha_{\lambda\mu} Y_{\lambda\mu}(\hat{r}_\alpha) \right) \quad (5.2)$$

and expanded into powers ( $t$ ) of  $\sum_{\lambda\mu} \alpha_{\lambda\mu} Y_{\lambda\mu}(\hat{r}_\alpha)$ .

The coupling between various channels is given by the matrix elements

$$\begin{aligned} \langle 1I | U_{\text{coupl}} | 1'I' \rangle &= \sum_L A(1, I, 1'I'; LJ) \\ \sum_t u_L^{(t)}(r) \langle I | Q_L^{(t)} | I' \rangle & \end{aligned} \quad (5.3)$$

where the factors  $A(1, I, 1'I', LJ)$  (depending on the partial waves of the incoming ( $l$ ) and scattered ( $l'$ ) particles, the nuclear spins  $I, I'$ , the channel spin  $J$  and multipolarity  $L$ ) are purely geometrical. The reduced matrix elements of the operators  $Q_L^{(t)}$  (operating only on target coordinates and built up by the  $\alpha_\lambda$ -operators coupled to the multipolarity  $L$ ) determine the strength of the transitions while the radial form factors  $u_L^{(t)} = v_L^{(t)} + iw_L^{(t)}$  are defined as derivatives ( $t$ ) of the shapes  $f(r_\alpha)$  and  $g(r_\alpha)$ . The relation of the reduced matrix elements  $\langle I | Q_L^{(t)} | I' \rangle$  to deformation

parameters  $\beta_{II}$ , of an anharmonic vibrational model is given elsewhere<sup>21</sup>. Taking the involved matrix elements or deformation parameters ( $\beta_{02}$ ,  $\beta_{24}$  and  $\beta_{04}$  in a  $0^+ - 2^+ - 4^+$  coupling scheme, e.g.<sup>21</sup>) as free parameters the model dependence is considerably reduced and the anharmonic vibrational model works just as a convenient parametrization of the form factors. Recently, in a further step of generalization rather flexible shapes of  $v_L(r)$  have been introduced<sup>15</sup> in inelastic alpha-particle scattering analyses. Results of such "model-independent" analyses of the coupling potentials (eq. 5.3) of  $^{50}\text{Ti}(\alpha, \alpha')$  and  $^{52}\text{Cr}(\alpha, \alpha')$  scattering are given in ref. 15.

Figs. 7-9 and Tables 4-6 compile results obtained with derivative shapes of  $f(r_\alpha, R_v, a_v)$  and  $g(r_\alpha, R_w, a_w)$  (restricted to second order  $t=2$ ). In general, the real as well as the imaginary part of  $U(\vec{r}_\alpha)$  are assumed to be nonspherical. Complex coupling proves to be important for inelastic alpha-particle scattering. The imaginary part of  $U(\vec{r}_\alpha)$  is described in the traditional manner by a deformed Saxon-Woods shape  $g(r_\alpha, R_w, a_w, \beta_L^{\text{imag}})$  with a geometry and deformation independent from the real part. When analyzing the  $2^+_1$  cross sections in a  $0^+ - 2^+$  coupling scheme, a  $\text{SW}^2$  form appears to be generally superior, not only for the diagonal potentials, but also for describing the inelastic coupling. However, in the case of  $3^-_1$  excitation different shapes of the diagonal potential ( $\text{SW}^2$  shape) and the coupling potential (SW derivative shape) lead to considerably better theoretical descriptions of the  $3^-_1$  cross sections (see Table 5). In contrast to DWBA which takes into account only the couplings to the ground state, the coupled channel calculations include automatically the competition of various reactions paths and the feedback of inelastic excitations to the optical potentials (see Fig. 6). Coulomb excitation has been included by a deformed Coulomb potential (with fixed deformation derived from measured  $B(\text{EL})$ -values). For the coupled channel calculations the Karlsruhe version of the Code ECIS has been used<sup>22</sup>.

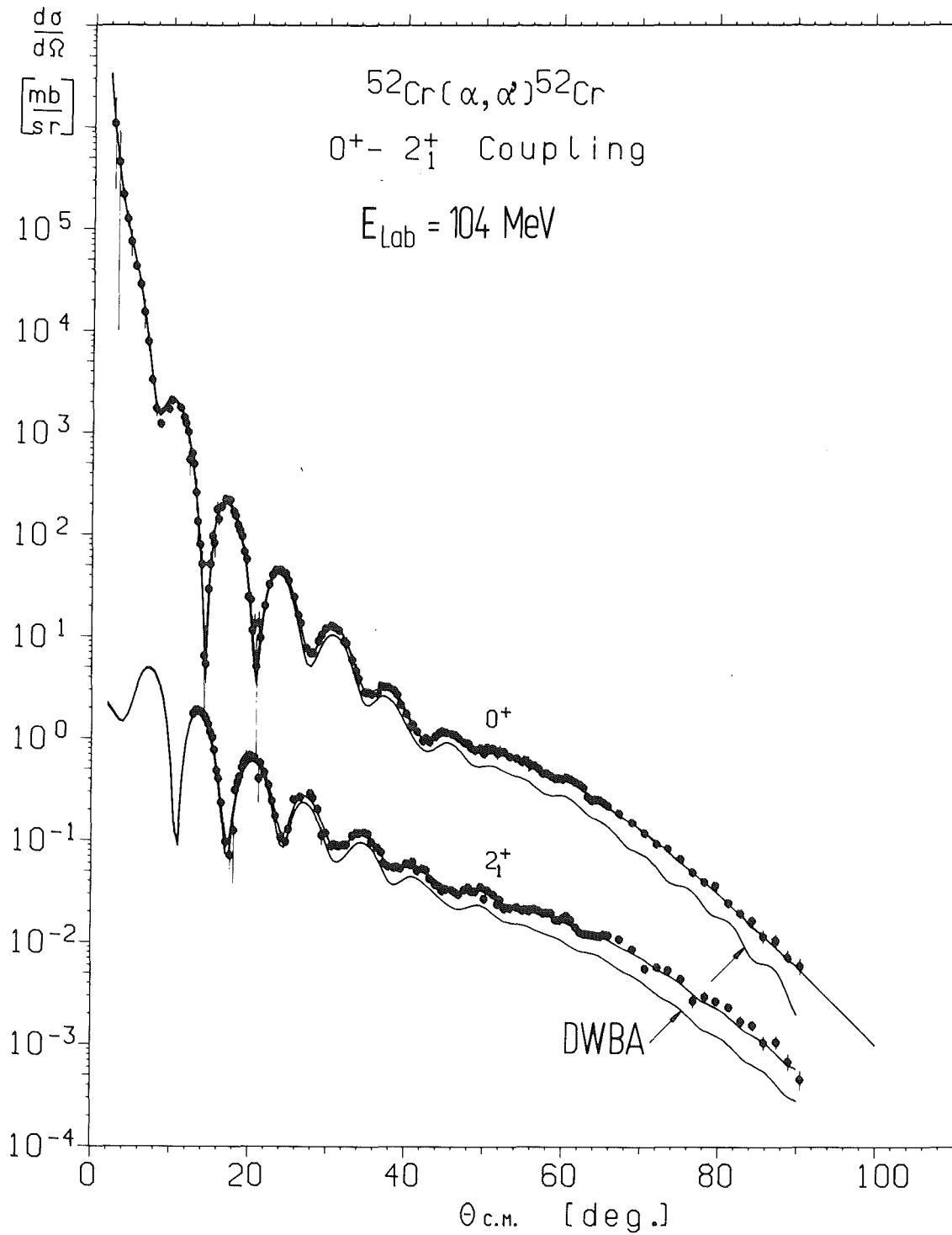


Fig. 7 Coupled channel analysis of  $^{52}\text{Cr}(\alpha, \alpha')$  scattering ( $0^+ - 2_1^+$ ) on the basis of a phenomenologically deformed optical potential. The first order DWBA prediction is shown for comparison.

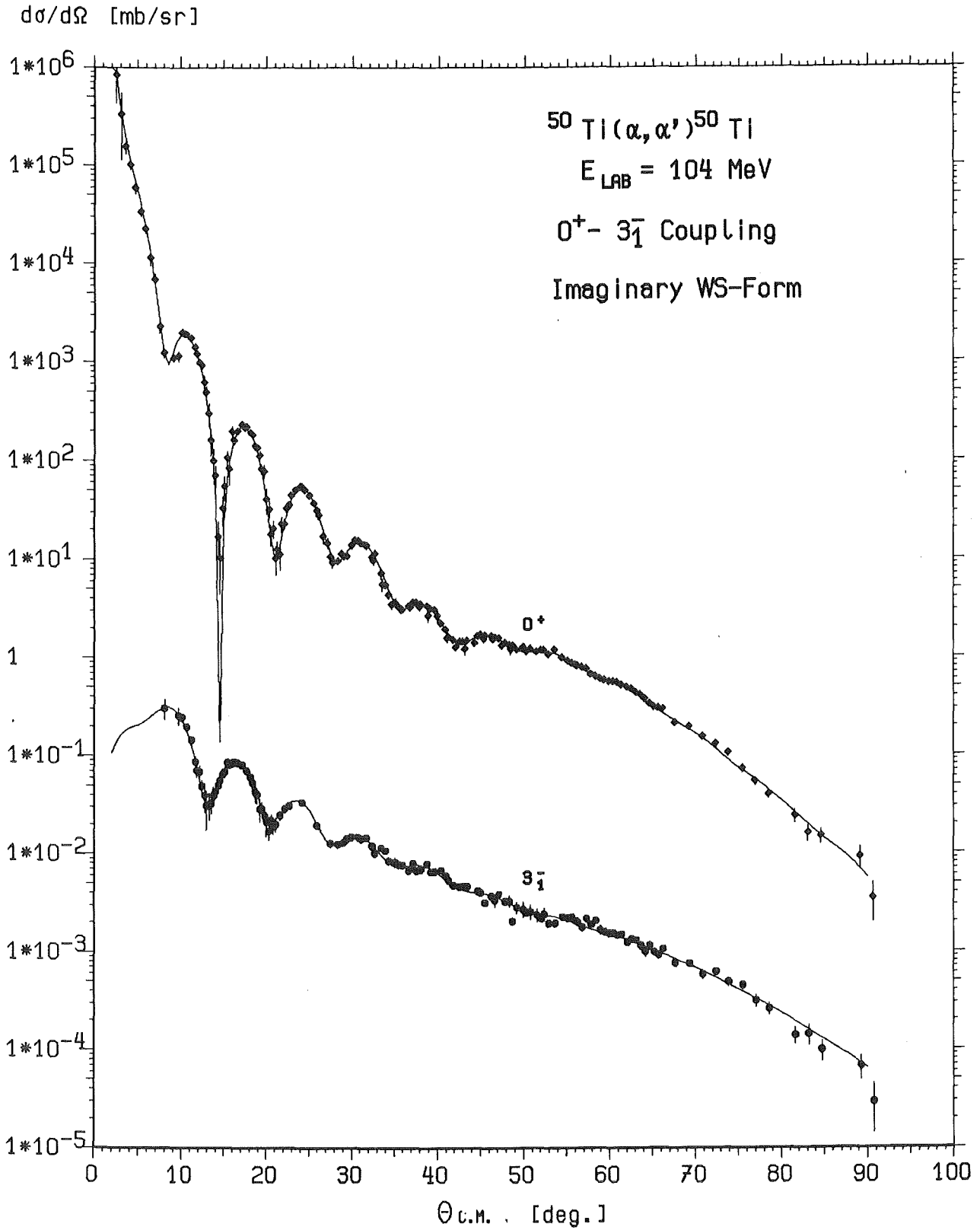


Fig. 8 Coupled channel analysis of the  $3_1^-$  excitation in  $^{50}\text{Ti}(\alpha, \alpha')$  scattering using different radial shapes of the real diagonal and derivative transition potentials (see Table 5).

Table 4 Extended optical potentials with  $SW^2$  radial shapes of the real part as derived from  $^{50}\text{Ti}(\alpha, \alpha')$  and  $^{52}\text{Cr}(\alpha, \alpha')$  differential cross sections

A	$V_O$ [MeV]	$R_V$ [fm]	$a_V$ [fm]	$W_O$ [MeV]	$R_W$ [fm]	$a_W$ [fm]	$\beta_L^{\text{real}}$	$\beta_L^{\text{imag}}$	$0^+$	$\chi^2/F$ I	total	Coupling
$^{50}\text{Ti}$	144.0	5.25	1.19	18.8	5.99	0.59	0.122	$= \beta_2^{\text{real}}$	2.2	4.2	3.2	$0^+-2_1^+$ L=2
	145.4	5.21	1.18	19.2	5.88	0.56	0.123	0.178	2.2	4.1	3.0	$0^+-3_1^-$ L=3
$^{52}\text{Cr}$	152.0	5.20	1.24	21.2	5.76	0.64	0.127	0.206	2.2	7.0	4.3	$0^+-2_1^+$ L=2
	156.6	5.12	1.20	21.8	5.40	0.65	0.112	$= \beta_3^{\text{real}}$	2.6	10.9	6.5	$0^+-3_1^-$ L=3

Table 5  $SW^2$  real diagonal potentials ( $V_O, R_V, a_V$ ) and SW derivative ( $V_O^{\text{trans}}, R_V^{\text{trans}}, a_V^{\text{trans}}$ ) transition potentials describing the  $0^+-3_1^-$  excitation in  $^{50}\text{Ti}$  and  $^{52}\text{Cr}$  by  $(\alpha, \alpha')$  scattering

A	$V_O/V_O^{\text{trans}}$ [MeV]	$R_V/R_V^{\text{trans}}$ [fm]	$a_V/a_V^{\text{trans}}$ [fm]	$W_O$ [MeV]	$r_w$ [fm]	$a_w$ [fm]	$\beta_3^{\text{real}}$	$\beta_3^{\text{imag}}$	$0^+$	$\chi^2/F$ 3	total	Coupling
$^{50}\text{Ti}$	148.9	5.16	1.20	19.7	5.81	0.56	0.133	0.255	1.7	2.2	1.9	$0^+-3_1^-$
	83.4	4.95	0.76									
$^{52}\text{Cr}$	165.4	5.00	1.26	23.9	5.39	0.66	0.09	0.51	1.4	3.6	2.5	$0^+-3_1^-$
	83.3	5.49	0.56									



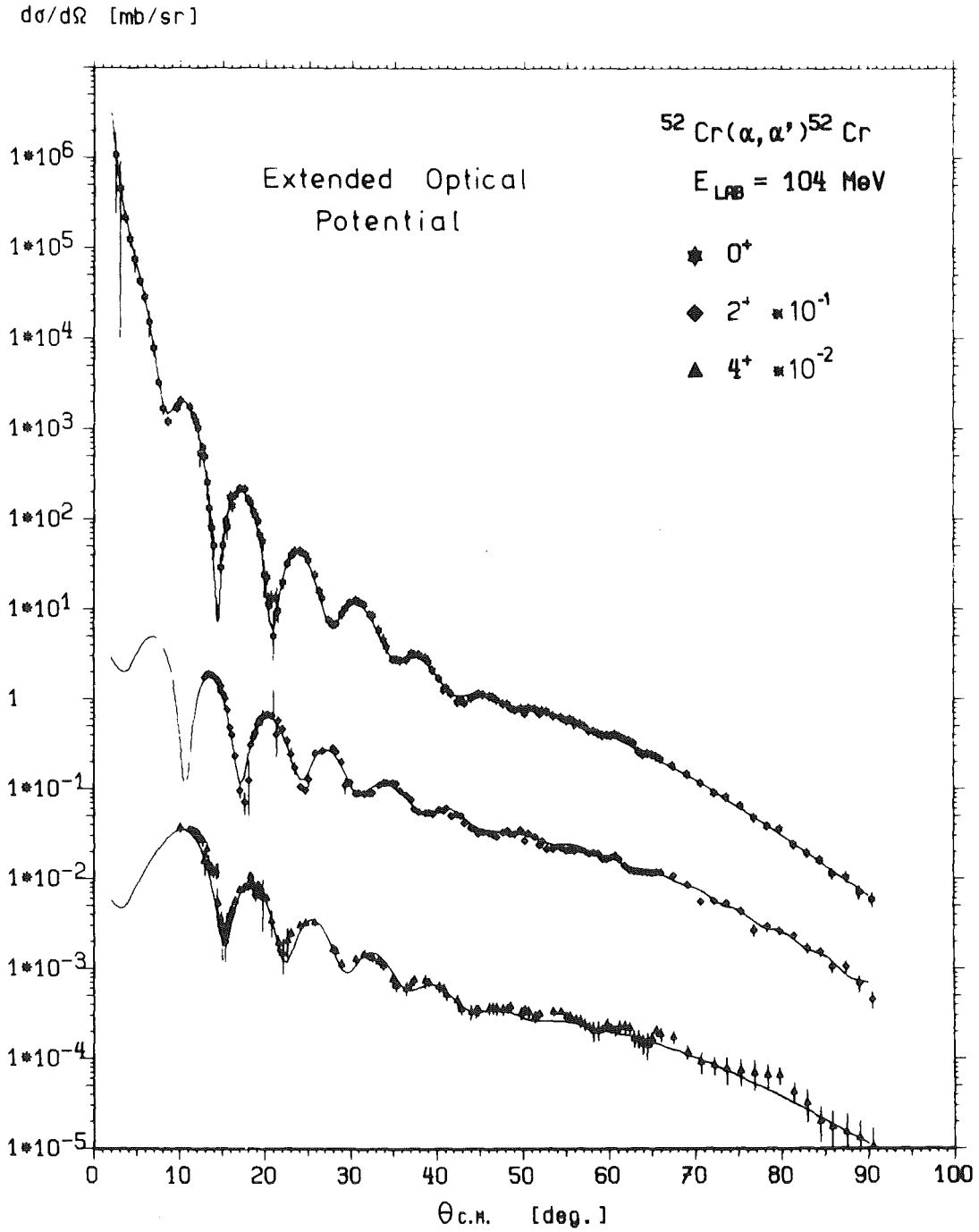


Fig. 9 Coupled channel analysis of  $^{52}\text{Cr}(\alpha, \alpha')$  scattering on the basis of a deformed optical potential and coupling the ground,  $2_1^+$  and  $4_1^+$  states.

Table 6 Extended optical potentials derived CC analysis of the  $0^+$ ,  $2_1^+$  and  $4_1^+$  differential cross section of  $^{50}\text{Ti}(\alpha, \alpha')$  and  $^{52}\text{Cr}(\alpha, \alpha')$  scattering

A	$V_O$	$r_V$	$a_V$	$W_O$	$r_W$	$a_W$	$\beta_{02}$	$\beta_{04}$	$\beta_{024}$	$-J_O/4A$	$\langle r_V^2 \rangle^{1/2}$	$\chi^2/F$		
	[MeV]	[fm]	[fm]	[MeV]	[fm]	[fm]				[MeV fm <sup>3</sup> ]	[fm]	0 <sup>+</sup>	2 <sup>+</sup>	4 <sup>+</sup>
$^{50}\text{Ti}$	143.5	1.43	1.17	18.6	1.61	0.57	0.12	0.06	0.075	311.4	4.48	1.9	5.7	2.1
$^{52}\text{Cr}$	151.8	1.39	1.20	22.3	1.51	0.72	0.13	0.05	0.075	303.02	4.47	2.8	6.3	1.7

Table 7 Folding model analysis with deformed Fermi distributions using (DD) and density independent (DI)

A	Proc.	$c_O$	$a_m$	$W_O$	$r_W$	$a_W$	$\beta_{02}^m$	$\beta_{04}^m$	$\beta_{24}^m$	$-J_O/4A$	$\langle r_m^2 \rangle^{1/2}$	$\chi^2/F$		
		[fm]	[fm]	[MeV]	[fm]	[fm]				[MeV fm <sup>3</sup> ]	[fm]	0 <sup>+</sup>	2 <sup>+</sup>	4 <sup>+</sup>
$^{50}\text{Ti}$	DD	1.04	0.522	18.1	1.58	0.634	0.124	0.009	0.075	297.3	3.542	2.5	4.1	3.5
$^{52}\text{Cr}$		1.08	0.463	20.7	1.54	0.682	0.121	0.08	0.075	295.7	3.566	2.1	2.7	2.2
$^{50}\text{Ti}$	DI	1.23	0.413	18.6	1.65	0.551	0.145	-	-	-	3.83	12.0	19.0	-
$^{52}\text{Cr}$		1.10	0.270	22.3	1.55	0.655	0.170	-	-	-	3.34	23.0	11.0	-

## 5.2 Deformed Folding Model

Folding models are applied in order to separate effects due to the properties of the probing projectile from the influence of the specific structure of the target nucleus. A natural extension of successful semi-microscopic descriptions of elastic scattering by single folding models is the generalization of eq. 4.1 to a deformed nucleon distribution  $\rho_m(\vec{r})$ , thus generating a deformed real potential. Such an approach has been applied in several cases (see for example refs. 16 and 23) specifying the effective interaction by a simple Gaussian form. Adopting a Fermi shape for the nucleon distribution the (permanent or dynamic) deformation is introduced (similarly to 5.2) by the angular dependence of the half-way radius

$$c_m(r) = c_0 (1 + \sum_{\lambda\mu} \alpha_{\lambda\mu}^{(m)}(\hat{r})) \quad (5.3)$$

Recent *elastic* alpha-particle scattering studies<sup>8,24,25</sup> have shown that a *density-dependent* effective interaction  $V_{\alpha N}$  is required when the data extend to larger angles beyond the diffraction region. We are interested to which extent saturation effects are also evident in *inelastic* cross sections and consider a Gaussian effective interaction

$$V_{\alpha N}(\vec{r}, \vec{r}_\alpha, \rho_m) = -V_0 \exp(-|\vec{r} - \vec{r}_\alpha|/a^2) \cdot f(\rho_m) \quad (5.4)$$

describing the density dependence by<sup>26</sup>

$$f(\rho_m) = 1 - \gamma \rho_m^{2/3} \quad (5.4b)$$

Introducing the parameter values

$$V_0 = 64.6 \text{ MeV} \quad a = 1.798 \text{ fm} \quad \gamma = 1.9 \text{ fm}^2$$

as obtained by a calibration<sup>8</sup> with elastic scattering from <sup>40</sup>Ca, and comparing with theoretical results based on a density-independent Gaussian interaction with usual parameter values<sup>16</sup>,

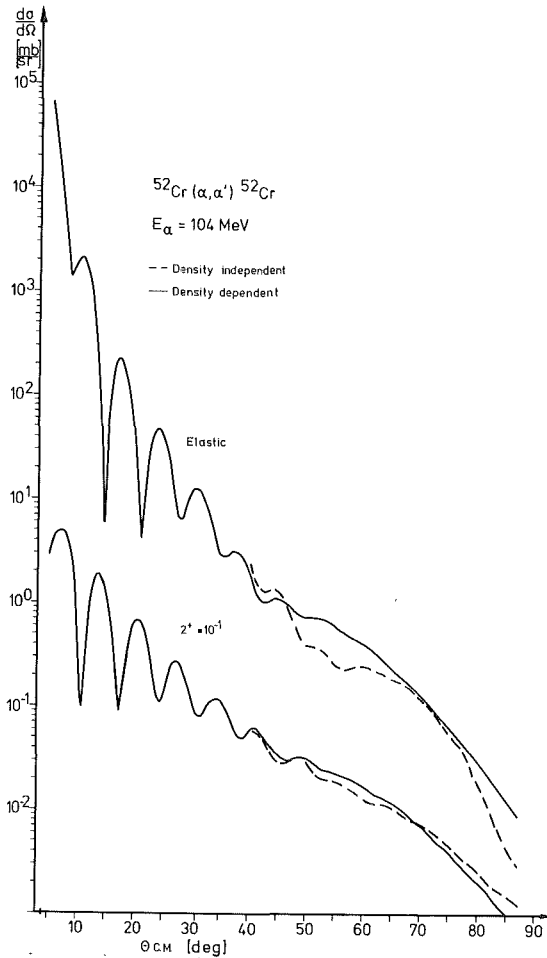


Fig. 10 Folding model description of elastic and inelastic scattering of 104 MeV alpha-particles using density-dependent (—) and density-independent effective interactions. The full lines reproduce the experimental data.

the density dependent version leads to considerably improved fits, in particular for large-angle scattering (Figs. 10 and 11). As calculations show, there is also little freedom in varying the parameter values of  $V_{\alpha N}$  as long as the experimental cross sections are well reproduced. The analysis started with parameter values ( $c_0, a_m$ ) of the (Fermi shaped) nuclear matter distributions comparable to charge distribution values<sup>27</sup>. Later on, the parameter values have been slightly varied due to possible differences of matter and charge distribution and explicit handling of deformation effects. For sake of simplicity, the deformation of the imaginary part has been taken to be identical with the deformation of the nuclear matter distribution.

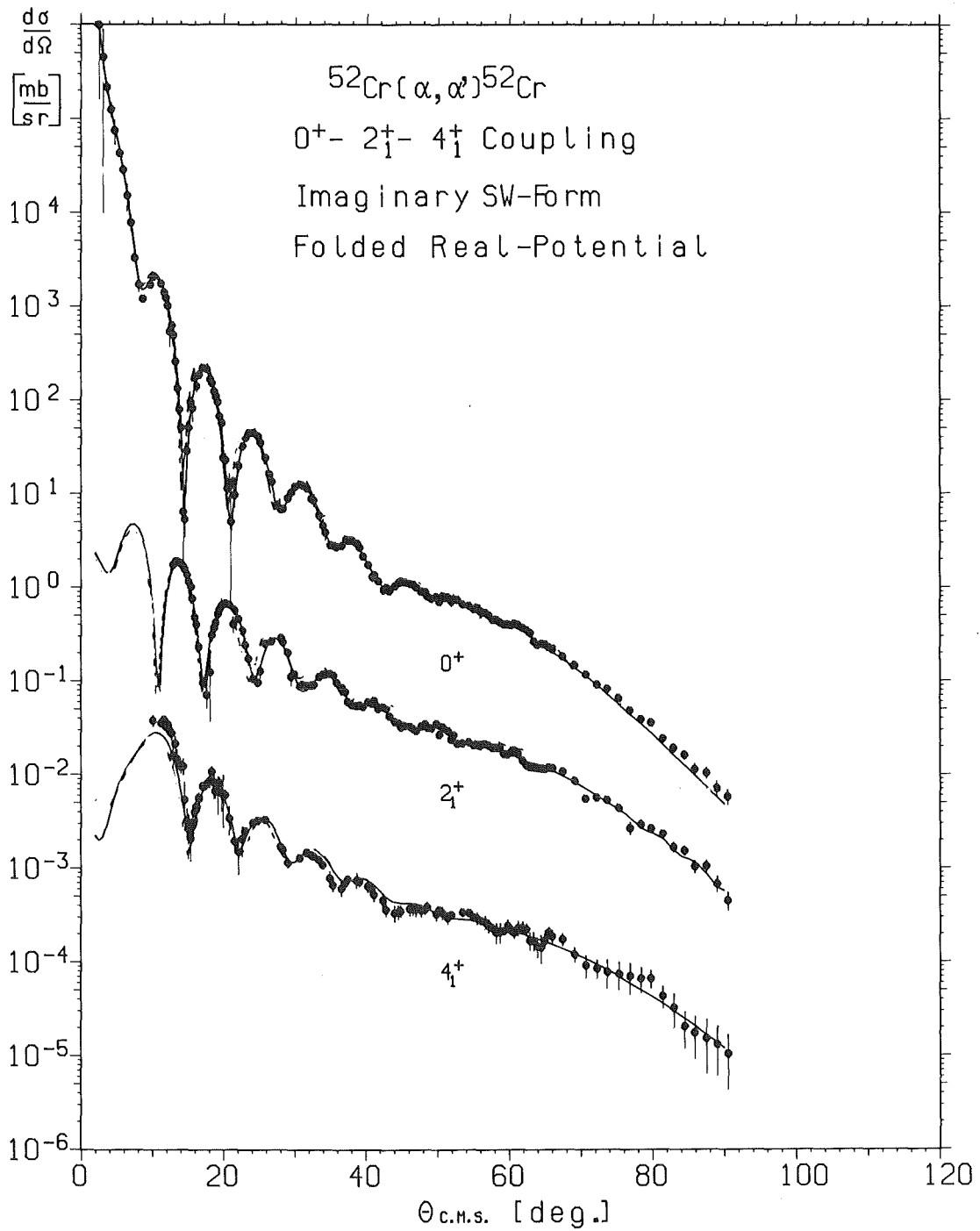


Fig. 11 Folding model description of elastic and inelastic scattering of 104 MeV alpha particles from  $^{52}\text{Cr}$  using a density-dependent alpha-particle-bound nucleon effective interaction

Though the density independent interaction generally fails (see Table 7) to reproduce the experimental cross sections over the full angular range, the best-fit values of the deformation parameters (fitting the diffraction region rather well) appear to be quite reasonable and consistent with  $(p, p')$  values. In contrast, the analysis based on a density dependent version of the folding model leads to a smaller deformation of the density distribution  $\rho_m$ , roughly equal to the deformation of the (real) potential. This feature is considered to be unreasonable. In fact, the resulting isoscalar transition rates are rather small and inconsistent with results from various other methods.

One reason of this discrepancy might be the use of an incorrect parametrization<sup>28</sup> of the density dependence (eq. 5.4 b) since, e.g. only the target density is entering. In addition, there is no guarantee that the deformation prescription such as eq. 5.3 is adequate to give the correct shape of the transition densities. This latter point has been extensively discussed by Satchler<sup>29</sup>. It is expected to be of importance just in cases when large angle scattering is probing deeper into the nucleus. These problems in applying a deformed folding model to inelastic alpha particle scattering have not been systematically studied so far. For the moment, we may conclude, that saturation effects seem to be important when describing inelastic scattering cross sections on the basis of a semi-microscopic folding model. However, the meaning of the deformation parameters, introduced by the standard procedure, remains unclear.

## 6. ISOSCALAR TRANSITION RATES AND DEFORMATION EFFECTS

The present analysis of inelastic scattering is restricted to derivative shapes of the coupling potentials and transition densities. However, as shown by more "model independent" analyses of the  $2_1^+$  and  $3_1^-$  state excitation, such "vibrational model" form factors are rather good approximations to realistic shapes, at least for cases considered here. This is pointed

out by the good agreement with isoscalar transition rates derived by a radial momenta analysis (RMA described in detail in refs. 15 and 30) of the coupling potentials obtained by more model dependent procedures. Since the "model independent" results<sup>15,31</sup> include realistic estimates of the uncertainties, we prefer to quote these  $B(IS, 0^+ - 2_1^+)$  and  $B(IS, 0^+ - 3_1^-)$  values when comparing with electromagnetic results\* (Tab.9). Due to the uncertainties indicated in sect. 5.2 we do not compare with results from explicit folding procedures. But it should be emphasized that only in the case of a (reliable) folding model analysis the deformation parameters could be expected to be representative for the nuclear mean square deformation. In the case of the vibrational model parametrization of the coupling potentials the  $\beta_L$  parameters (Tables 4-6) should be primarily considered as adjustable normalization of the coupling strengths. This role is particularly obvious in "decoupled" cases when the shapes of the coupling potentials are not deduced as being derivatives just of the diagonal parts (sect. 5.1). The quantities of interest which allow a meaningful discussion are mainly the resulting transition rates. Additionally, electromagnetic and RMA-values have been transformed into charge and matter distribution deformation of equivalent homogeneous distributions, using the relation

$$\langle \beta_L^2 \rangle = B(L) \cdot \left[ \frac{4\pi}{3Z} \frac{1}{R_{eq}^L} \right]^2 \quad (6.1)$$

with  $R_{eq}$  being the equivalent radius of the considered distribution.

It is interesting to note that the variations of the mean square deformation, which is contributing to the radius variation by

$$\delta \langle r^2 \rangle_\beta = \frac{5}{4\pi} \langle r_0^2 \rangle \sum \delta \langle \beta_L^2 \rangle \quad (6.2)$$

---

\* For a convenient comparison of electromagnetic and isoscalar transition rates,  $B(EL)$  and  $B(IS)$  are normalized to the same number of particles  $Z$ .

shows the same tendency with  $A = 48$  to  $A = 52$  as the experimental  $\delta\langle r_m^2 \rangle$  values (see Table 3). When evaluating\* eq. 6.2 only the lowest collective vibrations are considered as the high-lying collective states are expected to exhibit rather small fluctuations.

Table 8 Transition rates  $G_L$  (in single particle units) for the first excited  $2^+$ ,  $3^-$  and  $4^+$  states and nuclear mean square deformation

	$^{50}\text{Ti}$		$^{52}\text{Cr}$	
	EM	RMA	EM	RMA
$G_2$	$6.3 \pm 0.4^a$	$7.1 \pm 0.3$	$11.6 \pm 0.5^a$	$8.8 \pm 0.1$
$\langle \beta_2^2 \rangle_m^{1/2}$	0.17	0.19	0.20	0.19
$G_3$	-	$12.1 \pm 0.5$	$6.1 \pm 0.3^a$	$11.1 \pm 0.3$
$\langle \beta_3^2 \rangle_m^{1/2}$	-	0.24	0.14	0.23
$G_4$	-	$6.6^b$	$4.5 \pm 0.6^a$	$4.5^b$
$\langle \beta_4^2 \rangle_m^{1/2}$	-	0.16	0.10	0.13

<sup>a</sup> Ref.31

<sup>b</sup> Derived from coupling potentials (Tab. 6) with an uncertainty estimated to about 20 %.

\* The reference values  $\beta_L$  for  $^{48}\text{Ca}$  have been taken from ref. 33. Following Wagner et al.<sup>30</sup> these values, which are based on a zero-range procedure, have been rescaled by  $(\langle r^{L-1} \rangle_v / \langle r^{L-1} \rangle_m)^2$  where  $\langle r^{L-1} \rangle_{v,m}$  stand for the corresponding radial moments of the potential and matter distributions, respectively.



## 7. CONCLUDING REMARKS

Differential cross sections for elastic and inelastic 104-MeV alpha-particle scattering from  $^{48}\text{Ca}$ ,  $^{50}\text{Ti}$  and  $^{52}\text{Cr}$  have been presented and are used for determining precisely the strengths and radial shapes of the optical potentials. Looking for isotopic effects in the  $N = 28$  chain, mean square radii differences and isoscalar transition rates are extracted from the data. In contrast to the charge and proton radii, which are increasing when adding protons to the  $^{48}\text{Ca}$  core, the matter radii do not so and the mean square deformation (representing ground state fluctuations) appears to be slightly decreasing.

We thank Prof. Dr. G. Schatz for his encouraging interest in these studies and acknowledge the help of Dipl. math. J. Oehlschläger in solving computer problems.

REFERENCES

- 1 "What Do we Know about Radial Shape of Nuclei in the Ca Region", Proceed. Karlsruhe Internat. Discussion Meeting, May 2-4, 1979 (KfK 2830), eds. H. Rebel, H.J. Gils, and G. Schatz
- 2 F. Frosch, R. Hofstadter, J.S. McCarthy, G.K. Nöldeke, K.J. van Ostrum, M.R. Yearian, B.C. Clark, R. Herman and D.G. Ravenhall, Phys. Rev. 174 (1968) 1380
- 3 H.D. Wohlfahrt, E. Shera, M. Hoehn, Y. Yamazaki, G. Fricke and R. Steffen, Phys. Lett. 73B (1978) 131
- 4 H.D. Wohlfahrt, E.B. Shera, M.v. Hoehn, Y. Yamazaki, and R.M. Steffen, Phys. Rev. C 23 (1981) 533
- 5 F. Träger, Z. Physik A 299 (1981) 33
- 6 A. Andl, K. Bekk, S. Göring, A. Hanser, G. Nowicki, H. Rebel, G. Schatz and R.C. Thompson, Phys. Rev. C26 (1981) 2194
- 7 L. Ray, Phys. Rev. C19 (1979) 1855
- 8 H.J. Gils, E. Friedman, H. Rebel, J. Buschmann, S. Zagromski, H. Klewe-Nebenius, B. Neumann, R. Pesl and G. Bechtold, Phys. Rev. C21 (1980) 1239  
H.J. Gils, E. Friedman, Z. Majka and H. Rebel, Phys. Rev. C21 (1980) 1245
- 9 E. Friedman, H.J. Gils and H. Rebel, Phys. Rev. C25 (1982) 1551
- 10 E. Friedman and C.J. Batty, Phys. Rev. C17 (1978) 34
- 11 N. Vinh Mau, Phys. Lett. 71B (1977) 5  
N. Vinh Mau, in "The  $\alpha$ -Nucleus Interaction", Proc. of the 2nd Louvain-Cracow Seminar, ed. G. Gregoire, and K. Grotowski, Louvain-la-Neuve, Belgium, 1978
- 12 E. Friedman, H.J. Gils, H. Rebel and R. Pesl, Nucl. Phys. A363 (1981) 137
- 13 D.A. Goldberg and S.M. Smith, Phys. Rev. Lett. 29 (1972) 500
- 14 P.G. Reinhard and D. Drechsel, Z. Phys. A290 (1979) 85
- 15 H. Rebel, R. Pesl, H.J. Gils and E. Friedman, Nucl. Phys. A368 (1981) 61

- 16 H. Rebel, G. Hauser, G.W. Schweimer, G. Nowicki,  
W. Wiesner, and D. Hartmann, Nucl. Phys. A218 (1974) 13  
H. Rebel, Z. Physik A277 (1976) 35
- 17 R. Pesl, KfK-Report 3242 (1982)
- 18 D.A. Goldberg, Phys. Lett. 55B (1975) 59  
Z. Majka and T. Srokowski, Acta Physica Polonica  
B9 (1978) 75
- 19 H.J. Gils, KfK 3063 (1980)
- 20 H.J. Gils, E. Friedman and H. Rebel  
in preparation
- 21 T. Tamura, Progr. Theor. Phys. Suppl. 37 and 38 (1966)  
383  
H. Rebel, R. Löhken, G.W. Schweimer, G. Schatz and  
G. Hauser, Z. Phys. 256 (1972) 258
- 22 G.W. Schweimer and J. Raynal, private communications
- 23 H.J. Gils, H. Rebel, J. Buschmann, H. Klewe-Nebenius,  
G.P. Nowicki and W. Nowatzke, Z.Phys. A249 (1976)  
55
- 24 Z. Majka, H.J. Gils and H. Rebel, Z. Physik A288  
(1978) 139
- 25 A.M. Kobos, B.A. Brown, P.E. Hodgson, G.R. Satchler  
and A. Budzanowski, Oxford University Preprint 15/82
- 26 W.D. Myers, Nucl. Phys. A204 (1973) 465
- 27 J. Heisenberg, R. Hofstadter, J.S. McCarthy, R. Herman,  
B.C. Clark and D.G. Ravenhall, Phys. Rev. C6 (1972) 381.
- 28 H.J. Gils to be published
- 29 G. R. Satchler, Phys. Lett. 39B (1972) 495
- 30 G.J. Wagner, P. Grabmayr and H.R. Schmidt,  
Phys. Lett. 113B (1982) 447
- 31 V. Corcalciuc, R. Pesl, H. Rebel and H.J. Gils  
KfK 3377 (1982) - Journ. Phys.G : Nucl. Phys. (in press)
- 32 P.M. Endt, Atomic and Nuclear Data Tables 23, 6, 547
- 33 A. M. Bernstein, Advances in nuclear physics Vol.3, p.325 ff  
ed. M. Baranger and E. Vogt (Plenum, 1969 New York)

## APPENDIX: NUMERICAL TABLE OF EXPERIMENTAL CROSS SECTIONS

SCATTERING OF 4-HE PARTICLES ON TI-50

ELAB = 104.000 MEV    Q = 0.0 MEV    I = 0 +  
 ECM = 96.291 MEV    K = 4.1322/FERMI    ETA = 1.48297

LABORATORY DATA			RUTHERFORD	CM DATA		
THETA DEGREE	SIGMA MB/SR	DSIGMA %	SIGMA/SR	THETA DEGREE	SIGMA MB/SR	DSIGMA MB/SR
2.34	9.753E+05	49.1	6.166E-01	2.53	8.330E+05	4.094F+05
2.84	3.881E+05	68.6	5.323E-01	3.07	3.315E+05	2.275E+05
3.34	1.819E+05	21.6	4.772E-01	3.61	1.554E+05	3.350E+04
3.85	1.186E+05	13.7	5.474E-01	4.16	1.013E+05	1.390E+04
4.36	6.885E+04	15.6	5.228E-01	4.71	5.882E+04	9.176E+03
4.95	3.953E+04	14.0	5.000E-01	5.36	3.378E+04	4.737E+03
5.45	2.633E+04	14.6	4.892E-01	5.90	2.250E+04	3.285E+03
5.95	1.344E+04	22.1	3.547E-01	6.44	1.149E+04	2.535E+03
6.45	8.066E+03	19.5	2.938E-01	6.98	6.895E+03	1.344E+03
6.95	2.704E+03	27.8	1.327E-01	7.52	2.312E+03	6.431E+02
7.45	1.455E+03	13.6	9.426E-02	8.06	1.244E+03	1.688E+02
8.45	1.291E+03	4.4	1.383E-01	9.14	1.104E+03	4.830E+01
8.95	1.345E+03	14.4	1.813E-01	9.68	1.151E+03	1.663E+02
9.34	2.329E+03	8.7	3.722E-01	10.10	1.993E+03	1.743E+02
9.65	2.246E+03	3.3	4.088E-01	10.44	1.922E+03	6.260E+01
9.84	2.237E+03	1.5	4.402E-01	10.64	1.915E+03	2.833E+01
10.34	2.039E+03	4.8	4.890E-01	11.18	1.746E+03	8.408E+01
10.75	1.651E+03	9.9	4.674E-01	11.63	1.414E+03	1.402E+02
10.95	1.418E+03	10.5	4.272E-01	11.84	1.214E+03	1.279E+02
11.25	1.155E+03	8.9	3.875E-01	12.17	9.889E+02	8.826E+01
11.45	1.078E+03	10.6	3.882E-01	12.38	9.236E+02	9.763E+01
11.75	7.247E+02	20.9	2.893E-01	12.71	6.209E+02	1.297E+02
11.95	5.723E+02	19.2	2.444E-01	12.92	4.904E+02	9.422E+01
12.25	3.491E+02	35.1	1.645E-01	13.25	2.992E+02	1.050E+02
12.45	1.862E+02	41.2	9.362E-02	13.46	1.596E+02	6.576E+01
12.75	1.154E+02	36.9	6.376E-02	13.79	9.889E+01	3.650E+01
12.95	8.201E+01	33.4	4.824E-02	14.00	7.032E+01	2.346E+01
13.25	1.973E+01	74.4	1.271E-02	14.33	1.692E+01	1.258E+01
13.45	1.196E+01	77.2	8.181E-03	14.54	1.026E+01	7.919E+00
13.75	3.818E+01	43.8	2.851E-02	14.87	3.275E+01	1.475E+01
13.95	6.355E+01	37.6	5.026E-02	15.08	5.452E+01	2.051E+01
14.25	1.235E+02	20.7	1.063E-01	15.41	1.060E+02	2.193E+01
14.45	9.629E+01	43.3	8.761E-02	15.62	8.264E+01	3.580E+01
14.75	2.260E+02	20.7	2.230E-01	15.95	1.940E+02	4.016E+01
14.95	1.855E+02	12.5	1.933E-01	16.16	1.593E+02	1.998E+01
15.33	2.306E+02	6.4	2.656E-01	16.5P	1.980E+02	1.263E+01
15.82	2.686E+02	3.8	3.509E-01	17.11	2.308E+02	8.864E+00
16.15	2.497E+02	4.2	3.536E-01	17.46	2.146E+02	9.115E+00
16.34	2.560E+02	3.5	3.797E-01	17.66	2.200E+02	7.754E+00
16.75	2.208E+02	4.7	3.612E-01	18.10	1.898E+02	8.951E+00
16.95	2.113E+02	7.4	3.626E-01	18.32	1.817E+02	1.344E+01
17.25	1.619E+02	9.5	2.977E-01	18.64	1.392E+02	1.325E+01
17.45	1.557E+02	5.7	2.997E-01	18.86	1.339E+02	7.592E+00
17.75	1.294E+02	15.2	2.665E-01	19.18	1.113E+02	1.692E+01
17.95	9.504E+01	14.3	2.047E-01	19.40	8.179E+01	1.170E+01
18.25	9.066E+01	19.7	2.085E-01	19.72	7.804E+01	1.539E+01
18.45	4.693E+01	39.1	1.127E-01	19.94	4.040E+01	1.578E+01
18.75	3.707E+01	25.2	9.489E-02	20.26	3.192E+01	8.046E+00
18.95	2.088E+01	31.6	5.575E-02	20.48	1.798E+01	5.686E+00
19.25	2.367E+01	23.9	6.725E-02	20.80	2.039E+01	4.868E+00
19.45	1.196E+01	44.0	3.543E-02	21.02	1.031E+01	4.541E+00
19.65	1.469E+01	19.4	4.529E-02	21.23	1.266E+01	2.451E+00
19.95	1.294E+01	40.6	4.238E-02	21.56	1.116E+01	4.531E+00
20.15	2.612E+01	21.4	8.896E-02	21.77	2.252E+01	4.821E+00
20.45	2.649E+01	16.1	9.576E-02	22.09	2.285E+01	3.678E+00
20.65	3.778E+01	14.7	1.418E-01	22.31	3.259E+01	4.778E+00
20.95	4.121E+01	11.1	1.637E-01	22.63	3.556E+01	3.951E+00
21.15	5.122E+01	10.5	2.113E-01	22.85	4.421E+01	4.648E+00
21.65	5.810E+01	4.8	2.629E-01	23.39	5.017E+01	2.411E+00
22.15	6.299E+01	2.5	3.119E-01	23.92	5.442E+01	1.380E+00
22.34	6.251E+01	2.0	3.202E-01	24.13	5.402E+01	1.094E+00
22.65	5.828E+01	4.6	3.152E-01	24.46	5.039E+01	2.308E+00
23.15	5.123E+01	6.0	3.020E-01	25.00	4.431E+01	2.665E+00
23.65	4.248E+01	8.8	2.724E-01	25.54	3.676E+01	3.248E+00
23.95	3.610E+01	8.1	2.433E-01	25.86	3.125E+01	2.520E+00
24.15	3.243E+01	11.6	2.259E-01	26.08	2.808E+01	3.270E+00
24.65	1.978E+01	16.9	1.494E-01	26.61	1.714E+01	2.890E+00
25.15	1.684E+01	13.6	1.318E-01	27.15	1.460E+01	1.989E+00
25.45	1.222E+01	14.0	1.047E-01	27.47	1.060E+01	1.486E+00
25.65	1.064E+01	11.1	9.398E-02	27.69	9.233E+00	1.024E+00
26.24	1.100E+01	4.9	1.063E-01	28.33	9.550E+00	4.641E-01
26.65	1.314E+01	5.7	1.348E-01	28.76	1.141E+01	6.477E-01
26.91	1.237E+01	2.2	1.318E-01	29.04	1.075E+01	2.372E-01
27.24	1.243E+01	4.8	1.389E-01	29.39	1.080E+01	5.224E-01
27.74	1.598E+01	5.7	1.919E-01	29.93	1.390E+01	7.935E-01
28.15	1.796E+01	3.3	2.285E-01	30.37	1.563E+01	5.112E-01
28.45	1.778E+01	2.1	2.358E-01	30.69	1.548E+01	3.187E-01
28.73	1.693E+01	2.4	2.333E-01	30.99	1.474E+01	3.490E-01
29.15	1.618E+01	4.2	2.360E-01	31.44	1.410E+01	5.964E-01
29.34	1.588E+01	3.7	2.376E-01	31.65	1.384E+01	5.121E-01
29.95	1.222E+01	7.4	1.982E-01	32.30	1.066E+01	7.839E-01

30.12	1.119E+01	13.8	1.857E-01	32.48	9.767E+00	1.344E+00
30.25	1.303E+01	12.0	2.197E-01	32.62	1.137E+01	1.362E+00
30.95	8.266E+00	17.3	1.524E-01	33.37	7.220E+00	1.250E+00
31.10	6.359E+00	17.4	1.195E-01	33.53	5.556E+00	9.674E-01
31.45	6.217E+00	5.9	1.220E-01	33.91	5.434E+00	3.201E-01
31.75	4.960E+00	10.6	1.010E-01	34.23	4.337E+00	4.605E-01
32.10	3.939E+00	10.2	8.370E-02	34.60	3.446E+00	3.522E-01
32.45	4.150E+00	3.8	9.200E-02	34.97	3.633E+00	1.388E-01
32.84	3.736E+00	4.6	8.675E-02	35.39	3.272E+00	1.500E-01
33.10	3.507E+00	5.2	8.398E-02	35.67	3.073E+00	1.602E-01
33.25	3.536E+00	2.2	8.617E-02	35.83	3.099E+00	6.745E-02
33.95	3.768E+00	3.0	9.957E-02	36.58	3.306E+00	9.788E-02
34.10	3.677E+00	7.6	9.885E-02	36.74	3.227E+00	2.447E-01
34.45	4.155E+00	3.4	1.162E-01	37.11	3.648E+00	1.225E-01
34.75	4.142E+00	2.9	1.198E-01	37.43	3.639E+00	1.047E-01
35.10	3.741E+00	6.8	1.125E-01	37.81	3.288E+00	2.250E-01
35.25	3.992E+00	4.1	1.220E-01	37.97	3.510E+00	1.446E-01
35.95	3.782E+00	10.4	1.248E-01	38.71	3.329E+00	3.479E-01
36.10	3.041E+00	18.1	1.019E-01	38.87	2.677E+00	4.847E-01
36.34	3.566E+00	5.3	1.227E-01	39.13	3.141E+00	1.653E-01
36.75	3.465E+00	8.0	1.245E-01	39.57	3.054E+00	2.429E-01
37.10	2.997E+00	13.5	1.117E-01	39.94	2.643E+00	3.578E-01
37.45	2.530E+00	7.3	9.772E-02	40.31	2.232E+00	1.626E-01
37.95	2.190E+00	11.1	8.904E-02	40.84	1.934E+00	2.153E-01
38.10	1.799E+00	12.8	7.426E-02	41.00	1.589E+00	2.036E-01
38.25	1.832E+00	3.5	7.679E-02	41.16	1.619E+00	5.723E-02
38.75	1.710E+00	4.7	7.533E-02	41.70	1.512E+00	7.074E-02
39.10	1.449E+00	8.5	6.607E-02	42.07	1.282E+00	1.088E-01
39.45	1.644E+00	3.6	7.761E-02	42.44	1.456E+00	5.238E-02
39.84	1.633E+00	4.7	8.005E-02	42.85	1.447E+00	6.788E-02
40.10	1.378E+00	16.6	6.927E-02	43.13	1.222E+00	2.031E-01
40.25	1.668E+00	9.1	8.503E-02	43.29	1.479E+00	1.340E-01
41.10	1.581E+00	6.7	8.731E-02	44.19	1.404E+00	9.389E-02
41.45	1.863E+00	4.0	1.063E-01	44.56	1.656E+00	6.631E-02
41.75	1.915E+00	3.2	1.123E-01	44.88	1.703E+00	5.513E-02
42.10	1.732E+00	8.2	1.049E-01	45.25	1.541E+00	1.269E-01
42.25	1.888E+00	4.3	1.159E-01	45.41	1.680E+00	7.304E-02
42.95	1.849E+00	4.1	1.208E-01	46.16	1.648E+00	6.767E-02
43.10	1.708E+00	6.8	1.131E-01	46.32	1.523E+00	1.031E-01
43.34	1.785E+00	5.9	1.207E-01	46.57	1.592E+00	9.351E-02
43.75	1.753E+00	3.7	1.229E-01	47.00	1.565E+00	5.764E-02
44.10	1.481E+00	8.7	1.070E-01	47.37	1.323E+00	1.152E-01
44.45	1.571E+00	2.3	1.170E-01	47.75	1.404E+00	3.175E-02
44.95	1.496E+00	8.1	1.162E-01	48.27	1.338E+00	1.081E-01
45.10	1.343E+00	13.2	1.057E-01	48.43	1.202E+00	1.586E-01
45.25	1.481E+00	6.0	1.180E-01	48.59	1.326E+00	7.927E-02
45.75	1.347E+00	5.7	1.119E-01	49.12	1.207E+00	6.921E-02
46.45	1.429E+00	6.8	1.257E-01	49.86	1.282E+00	8.780E-02
46.84	1.286E+00	3.4	1.168E-01	50.27	1.155E+00	3.947E-02
47.25	1.361E+00	5.0	1.277E-01	50.71	1.223E+00	6.114E-02
47.95	1.274E+00	6.2	1.264E-01	51.44	1.147E+00	7.148E-02
48.45	1.309E+00	1.4	1.349E-01	51.97	1.179E+00	1.630E-02
48.75	1.310E+00	5.5	1.383E-01	52.29	1.181E+00	6.531E-02
49.25	1.193E+00	2.8	1.309E-01	52.81	1.077E+00	2.984E-02
49.95	1.315E+00	2.8	1.521E-01	53.55	1.189E+00	3.378E-02
50.77	1.098E+00	3.0	1.350E-01	54.41	9.945E-01	3.019E-02
51.41	1.014E+00	2.1	1.305E-01	55.09	9.193E-01	1.927E-02
51.84	9.677E-01	2.9	1.285E-01	55.54	8.783E-01	2.583E-02
52.25	9.258E-01	2.2	1.266E-01	55.97	8.410E-01	1.819E-02
52.45	9.051E-01	3.1	1.256E-01	56.18	8.226E-01	2.511E-02
52.95	8.755E-01	2.1	1.258E-01	56.71	7.966E-01	1.677E-02
53.45	8.458E-01	3.4	1.259E-01	57.23	7.704E-01	2.630E-02
53.95	7.397E-01	4.4	1.139E-01	57.75	6.745E-01	2.941E-02
54.45	7.030E-01	2.7	1.121E-01	58.28	6.418E-01	1.726E-02
54.95	6.710E-01	3.6	1.106E-01	58.80	6.133E-01	2.184E-02
55.45	6.390E-01	3.4	1.089E-01	59.33	5.847E-01	2.009E-02
55.95	6.201E-01	2.3	1.093E-01	59.85	5.681E-01	1.292E-02
56.40	6.147E-01	2.1	1.115E-01	60.31	5.637E-01	1.164E-02
56.84	6.078E-01	3.3	1.135E-01	60.78	5.580E-01	1.853E-02
57.34	5.713E-01	3.6	1.102E-01	61.30	5.251E-01	1.890E-02
57.95	5.405E-01	3.2	1.083E-01	61.94	4.975E-01	1.581E-02
58.45	5.181E-01	3.7	1.072E-01	62.46	4.775E-01	1.771E-02
58.95	4.727E-01	3.9	1.008E-01	62.98	4.361E-01	1.713E-02
59.45	4.495E-01	4.1	9.888E-02	63.50	4.152E-01	1.707E-02
59.95	4.077E-01	4.7	9.247E-02	64.02	3.771E-01	1.771E-02
60.45	3.660E-01	5.0	8.554E-02	64.54	3.389E-01	1.694E-02
60.95	3.382E-01	4.0	8.145E-02	65.06	3.136E-01	1.250E-02
61.45	3.288E-01	4.0	8.154E-02	65.58	3.052E-01	1.224E-02
61.95	3.198E-01	4.4	8.166E-02	66.10	2.972E-01	1.302E-02
63.34	2.303E-01	4.7	6.370E-02	67.54	2.148E-01	1.008E-02
64.95	2.082E-01	4.2	6.300E-02	69.21	1.950E-01	8.168E-03
66.45	1.651E-01	5.4	5.418E-02	70.76	1.552E-01	8.415E-03
67.95	1.378E-01	4.7	4.895E-02	72.31	1.301E-01	6.166E-03
69.34	1.124E-01	6.6	4.287E-02	73.74	1.065E-01	6.994E-03
70.95	7.716E-02	7.6	3.188E-02	75.40	7.341E-02	5.546E-03
72.45	5.697E-02	9.2	2.531E-02	76.93	5.442E-02	4.982E-03
73.95	4.156E-02	9.5	1.981E-02	78.47	3.986E-02	3.796E-03
76.95	2.486E-02	14.7	1.357E-02	81.53	2.404E-02	3.523E-03
78.45	1.652E-02	17.7	9.625E-03	83.06	1.604E-02	2.843E-03
79.95	1.540E-02	16.5	9.563E-03	84.58	1.502E-02	2.480E-03
84.45	9.307E-03	25.0	6.923E-03	89.13	9.193E-03	2.296E-03
85.95	3.520E-03	43.5	2.772E-03	90.64	3.492E-03	1.519E-03

SCATTERING OF 4-HE PARTICLES ON TI-50

ELAB = 104.000 MEV    Q = -1.555 MEV    I = 2 +  
 ECM = 94.736 MEV    K = 4.0987/FERMI    ETA = 1.37050

LABORATORY DATA			CM DATA		
THETA DEGREE	SIGMA MB/SR	DSIGMA %	THETA DEGREE	SIGMA MB/SR	DSIGMA MB/SR
9.65	1.997E+00	54.8	10.45	1.707E+00	9.352E-01
9.84	3.763E+00	23.3	10.65	3.217E+00	7.506E-01
10.34	5.501E+00	15.3	11.19	4.704E+00	7.218E-01
10.70	8.935E+00	15.3	11.58	7.642E+00	1.169E+00
10.95	1.291E+01	9.4	11.85	1.104E+01	1.040E+00
11.20	1.384E+01	7.0	12.12	1.184E+01	8.261E-01
11.45	1.498E+01	7.6	12.39	1.282E+01	9.758E-01
11.72	1.577E+01	9.8	12.68	1.350E+01	1.324E+00
11.95	1.954E+01	10.2	12.93	1.672E+01	1.700E+00
12.20	2.215E+01	5.2	13.21	1.896E+01	9.901E-01
12.45	2.271E+01	5.8	13.47	1.944E+01	1.121E+00
12.71	2.357E+01	2.8	13.75	2.018E+01	5.568E-01
12.95	2.377E+01	5.0	14.01	2.036E+01	1.023E+00
13.22	2.340E+01	3.7	14.30	2.004E+01	7.469E-01
13.45	2.158E+01	5.2	14.55	1.849E+01	9.705E-01
13.72	2.067E+01	6.0	14.84	1.771E+01	1.054E+00
13.95	1.798E+01	9.5	15.09	1.541E+01	1.471E+00
14.23	1.538E+01	9.4	15.40	1.318E+01	1.238E+00
14.45	1.352E+01	17.5	15.63	1.159E+01	2.023E+00
14.73	7.000E+00	34.4	15.94	6.002E+00	2.063E+00
14.95	4.808E+00	25.7	16.17	4.123E+00	1.059E+00
15.31	2.685E+00	24.0	16.56	2.303E+00	5.528E-01
15.81	2.147E+00	15.3	17.10	1.842E+00	2.822E-01
16.15	2.101E+00	17.9	17.47	1.803E+00	3.224E-01
16.34	2.476E+00	15.9	17.67	2.126E+00	3.383E-01
16.68	2.791E+00	49.4	18.04	2.397E+00	1.185E+00
16.95	4.096E+00	17.2	18.33	3.518E+00	6.047E-01
17.18	5.046E+00	14.5	18.58	4.335E+00	6.266E-01
17.45	6.363E+00	10.0	18.87	5.467E+00	5.476E-01
17.69	6.949E+00	7.3	19.14	5.972E+00	4.336E-01
17.95	7.618E+00	6.2	19.41	6.548E+00	4.068E-01
18.21	7.838E+00	3.4	19.69	6.739E+00	2.287E-01
18.45	7.938E+00	7.1	19.95	6.826E+00	4.873E-01
18.68	8.306E+00	3.4	20.20	7.144E+00	2.438E-01
18.95	8.105E+00	5.6	20.49	6.973E+00	3.939E-01
19.19	8.274E+00	4.0	20.75	7.120E+00	2.883E-01
19.45	7.694E+00	6.5	21.03	6.623E+00	4.337E-01
19.65	7.531E+00	5.1	21.24	6.484E+00	3.301E-01
19.95	7.154E+00	6.8	21.57	6.161E+00	4.177E-01
20.15	6.426E+00	9.1	21.78	5.535E+00	5.064E-01
20.45	5.499E+00	10.9	22.11	4.738E+00	5.154E-01
20.65	4.724E+00	11.4	22.32	4.071E+00	4.633E-01
20.95	4.034E+00	12.4	22.65	3.477E+00	4.304E-01
21.15	3.377E+00	15.1	22.96	2.912E+00	4.395E-01
21.65	2.267E+00	16.0	23.40	1.956E+00	3.134E-01
22.15	1.666E+00	22.3	23.94	1.438E+00	3.211E-01
22.34	1.059E+00	34.5	24.14	9.143E-01	3.154E-01
22.65	1.637E+00	13.1	24.48	1.414E+00	1.853E-01
23.15	1.977E+00	8.6	25.01	1.708E+00	1.476E-01
23.65	2.162E+00	8.0	25.55	1.869E+00	1.504E-01
23.95	2.301E+00	14.1	25.88	1.990E+00	2.814E-01
24.15	3.097E+00	11.0	26.09	2.679E+00	2.950E-01
24.65	3.219E+00	6.9	26.63	2.786E+00	1.927E-01
25.15	3.932E+00	6.4	27.17	3.405E+00	2.174E-01
25.45	3.641E+00	4.5	27.49	3.154E+00	1.430E-01
25.65	3.792E+00	6.0	27.70	3.286E+00	1.975E-01
26.23	3.364E+00	6.2	28.33	2.917E+00	1.797E-01
26.65	2.650E+00	9.4	28.78	2.299E+00	2.157E-01
26.90	2.519E+00	6.3	29.05	2.186E+00	1.378E-01
27.23	2.020E+00	10.0	29.40	1.754E+00	1.760E-01
27.74	1.528E+00	7.2	29.94	1.327E+00	9.504E-02
28.15	1.534E+00	9.0	30.39	1.333E+00	1.205E-01
28.45	1.199E+00	9.3	30.71	1.043E+00	9.678E-02
28.68	1.234E+00	6.8	30.96	1.073E+00	7.256E-02
29.15	1.352E+00	11.0	31.46	1.177E+00	1.294E-01
29.34	1.370E+00	3.9	31.66	1.193E+00	4.634E-02
29.95	1.431E+00	5.5	32.32	1.247E+00	6.878E-02
30.23	1.389E+00	5.6	32.61	1.211E+00	6.734E-02
30.95	1.787E+00	8.4	33.39	1.559E+00	1.305E-01
31.10	1.577E+00	10.7	33.55	1.376E+00	1.466E-01
31.45	1.668E+00	5.0	33.92	1.457E+00	7.300E-02
31.75	1.762E+00	3.6	34.25	1.539E+00	5.600E-02
32.10	1.679E+00	6.6	34.62	1.468E+00	9.616E-02
32.45	1.682E+00	4.1	34.99	1.471E+00	5.969E-02

32.84	1.543E+00	4.1	35.41	1.350E+00	5.591E-02
33.10	1.546E+00	7.7	35.69	1.353E+00	1.045E-01
33.25	1.425E+00	5.8	35.85	1.248E+00	7.259E-02
33.95	1.322E+00	13.8	36.60	1.159E+00	1.604E-01
34.10	9.710E-01	21.7	36.76	8.513E-01	1.848E-01
34.45	1.045E+00	7.5	37.13	9.167E-01	6.871E-02
34.75	8.384E-01	7.9	37.45	7.358E-01	5.806E-02
35.10	8.054E-01	11.9	37.83	7.072E-01	8.422E-02
35.25	7.501E-01	6.1	37.99	6.588E-01	4.006E-02
35.95	7.383E-01	7.0	38.73	6.492E-01	4.514E-02
36.10	6.843E-01	9.6	38.89	6.019E-01	5.757E-02
36.34	6.803E-01	3.9	39.15	5.986E-01	2.354E-02
36.75	6.559E-01	6.5	39.59	5.775E-01	3.751E-02
37.10	6.350E-01	9.8	39.96	5.595E-01	5.468E-02
37.45	6.298E-01	5.5	40.33	5.552E-01	3.071E-02
37.95	6.726E-01	4.4	40.87	5.934E-01	2.594E-02
38.10	6.504E-01	10.1	41.03	5.740E-01	5.822E-02
38.25	7.126E-01	6.5	41.19	6.291E-01	4.061E-02
38.75	6.958E-01	3.4	41.72	6.148E-01	2.071E-02
39.10	7.012E-01	6.7	42.09	6.199E-01	4.140E-02
39.45	6.571E-01	4.7	42.46	5.813E-01	2.712E-02
39.84	6.779E-01	9.7	42.88	6.001E-01	5.817E-02
40.10	4.547E-01	27.2	43.15	4.027E-01	1.094E-01
40.25	5.195E-01	7.6	43.31	4.602E-01	3.502E-02
41.10	4.906E-01	9.4	44.22	4.353E-01	4.107E-02
41.45	5.241E-01	2.8	44.59	4.653E-01	1.292E-02
41.75	5.117E-01	3.7	44.91	4.546E-01	1.683E-02
42.10	5.323E-01	10.0	45.28	4.732E-01	4.718E-02
42.25	5.343E-01	2.1	45.44	4.751E-01	9.921E-03
42.95	4.933E-01	7.8	46.18	4.392E-01	3.424E-02
43.10	4.253E-01	12.1	46.34	3.788E-01	4.595E-02
43.34	4.046E-01	13.0	46.59	3.605E-01	4.669E-02
43.75	4.289E-01	3.9	47.03	3.825E-01	1.495E-02
44.10	3.853E-01	11.9	47.40	3.438E-01	4.100E-02
44.45	4.377E-01	3.7	47.77	3.909E-01	1.436E-02
44.95	4.216E-01	12.3	48.30	3.769E-01	4.630E-02
45.10	4.520E-01	11.5	48.46	4.042E-01	4.638E-02
45.25	4.695E-01	2.6	48.62	4.199E-01	1.072E-02
45.75	4.701E-01	8.9	49.15	4.209E-01	3.765E-02
46.45	4.631E-01	12.2	49.89	4.152E-01	5.048E-02
46.84	4.647E-01	2.3	50.30	4.170E-01	9.571E-03
47.25	4.540E-01	10.2	50.73	4.077E-01	4.141E-02
47.95	4.242E-01	10.5	51.47	3.815E-01	4.000E-02
48.45	4.505E-01	2.9	52.00	4.056E-01	1.165E-02
48.75	4.295E-01	9.7	52.32	3.869E-01	3.754E-02
49.25	3.717E-01	3.4	52.84	3.352E-01	1.143E-02
49.95	3.885E-01	2.9	53.58	3.509E-01	1.022E-02
50.77	4.120E-01	2.9	54.45	3.728E-01	1.094E-02
51.40	3.575E-01	2.8	55.11	3.239E-01	9.056E-03
51.84	3.495E-01	4.0	55.57	3.170E-01	1.268E-02
52.25	3.665E-01	3.3	56.00	3.327E-01	1.082E-02
52.45	3.841E-01	5.5	56.21	3.488E-01	1.916E-02
52.95	3.247E-01	4.6	56.73	2.952E-01	1.344E-02
53.45	3.027E-01	4.0	57.26	2.755E-01	1.099E-02
53.95	3.012E-01	5.0	57.78	2.745E-01	1.365E-02
54.45	3.024E-01	3.5	58.31	2.759E-01	9.520E-03
54.95	3.121E-01	4.8	58.83	2.851E-01	1.370E-02
55.45	2.860E-01	5.2	59.36	2.615E-01	1.371E-02
55.95	2.568E-01	4.3	59.88	2.351E-01	1.000E-02
56.40	2.756E-01	3.8	60.34	2.526E-01	9.566E-03
56.84	2.508E-01	4.9	60.81	2.301E-01	1.137E-02
57.34	2.443E-01	4.7	61.33	2.244E-01	1.051E-02
57.95	2.362E-01	4.3	61.97	2.173E-01	9.446E-03
58.45	2.211E-01	4.7	62.49	2.036E-01	9.570E-03
58.95	2.230E-01	4.9	63.01	2.056E-01	9.964E-03
59.45	1.951E-01	6.3	63.53	1.801E-01	1.128E-02
59.95	1.825E-01	5.9	64.05	1.687E-01	9.932E-03
60.45	1.769E-01	6.1	64.57	1.637E-01	9.949E-03
60.95	1.687E-01	5.1	65.10	1.563E-01	7.918E-03
61.45	1.650E-01	5.2	65.62	1.538E-01	8.050E-03
61.95	1.723E-01	5.2	66.13	1.601E-01	8.249E-03
63.34	1.447E-01	4.9	67.58	1.349E-01	6.650E-03
64.95	1.204E-01	5.3	69.25	1.127E-01	5.981E-03
66.45	8.523E-02	7.3	70.80	8.009E-02	5.828E-03
67.95	8.250E-02	5.7	72.34	7.783E-02	4.465E-03
69.34	7.130E-02	7.1	73.78	6.752E-02	4.818E-03
70.95	5.783E-02	7.5	75.43	5.500E-02	4.118E-03
72.45	4.455E-02	9.5	76.97	4.254E-02	4.022E-03
73.95	3.442E-02	9.5	78.51	3.300E-02	3.131E-03
76.95	2.161E-02	13.2	81.57	2.089E-02	2.755E-03
78.45	1.905E-02	20.8	83.09	1.850E-02	3.854E-03
79.95	1.541E-02	15.4	84.62	1.503E-02	2.319E-03
84.45	7.385E-03	26.1	89.17	7.294E-03	1.906E-03
85.95	5.385E-03	33.0	90.68	5.341E-03	1.765E-03

SCATTERING OF 4-HE PARTICLES ON TI-50

ELAB = 104.000 MEV      Q = -4.420 MEV      I = 3 -  
 ECM = 91.871 MEV      K = 4.0363/FERMI      ETA = 1.39171

LABORATORY DATA			CM DATA		
THETA DEGREE	SIGMA MB/SR	DSIGMA %	THETA DEGREE	SIGMA MB/SR	DSIGMA MB/SR
7.45	3.599E+01	23.5	8.07	3.067E+01	7.207E+00
8.95	2.975E+01	19.2	9.70	2.537E+01	4.876E+00
9.34	2.886E+01	9.4	10.12	2.461E+01	2.306E+00
9.84	2.315E+01	5.7	10.66	1.975E+01	1.135E+00
10.34	1.701E+01	10.5	11.20	1.451E+01	1.520E+00
10.75	8.728E+00	22.5	11.65	7.449E+00	1.673E+00
10.95	1.058E+01	13.1	11.86	9.031E+00	1.185E+00
11.25	8.104E+00	15.5	12.19	6.918E+00	1.073E+00
11.45	7.281E+00	12.9	12.41	6.216E+00	7.994E-01
11.75	9.321E+00	20.7	12.73	7.959E+00	1.651E+00
11.95	5.748E+00	37.2	12.95	4.909E+00	1.828E+00
12.25	9.241E+00	15.3	13.27	7.893E+00	1.205E+00
12.45	8.390E+00	11.8	13.49	7.167E+00	8.474E-01
12.75	1.047E+01	11.7	13.81	8.947E+00	1.046E+00
12.95	9.053E+00	10.6	14.03	7.736E+00	8.174E-01
13.25	7.791E+00	10.3	14.35	6.659E+00	6.831E-01
13.45	8.667E+00	10.1	14.57	7.408E+00	7.509E-01
13.75	1.030E+01	9.3	14.89	8.805E+00	8.155E-01
13.95	8.977E+00	15.3	15.11	7.676E+00	1.171E+00
14.25	5.559E+00	21.7	15.43	4.754E+00	1.031E+00
14.45	6.499E+00	10.5	15.65	5.559E+00	5.835E-01
14.75	5.780E+00	13.9	15.98	4.945E+00	6.892E-01
14.95	7.303E+00	11.5	16.19	6.249E+00	7.193E-01
15.29	6.309E+00	7.4	16.56	5.400E+00	3.982E-01
15.81	7.111E+00	5.0	17.13	6.089E+00	3.034E-01
16.33	5.933E+00	10.0	17.69	5.082E+00	5.066E-01
16.75	6.461E+00	18.5	18.14	5.536E+00	1.024E+00
16.95	5.087E+00	18.6	18.35	4.360E+00	8.093E-01
17.25	4.983E+00	23.4	18.68	4.272E+00	9.998E-01
17.45	3.499E+00	26.1	18.89	3.000E+00	7.833E-01
17.75	3.352E+00	26.7	19.22	2.875E+00	7.685E-01
17.95	2.479E+00	22.9	19.43	2.126E+00	4.864E-01
18.25	2.267E+00	22.0	19.76	1.945E+00	4.280E-01
18.45	1.985E+00	33.9	19.97	1.703E+00	5.777E-01
18.75	1.998E+00	19.2	20.30	1.715E+00	3.295E-01
18.95	1.974E+00	18.0	20.51	1.695E+00	3.056E-01
19.25	2.206E+00	15.2	20.84	1.894E+00	2.871E-01
19.45	2.330E+00	16.2	21.05	2.001E+00	3.247E-01
19.95	2.885E+00	11.9	21.59	2.479E+00	2.952E-01
20.45	3.933E+00	9.0	22.13	3.381E+00	3.026E-01
20.95	4.630E+00	6.2	22.67	3.983E+00	2.484E-01
22.34	3.872E+00	4.2	24.17	3.335E+00	1.392E-01
23.95	1.789E+00	9.8	25.90	1.544E+00	1.520E-01
25.45	1.246E+00	10.5	27.52	1.077E+00	1.130E-01
26.25	1.334E+00	8.3	28.38	1.154E+00	9.601E-02
26.90	1.630E+00	5.9	29.08	1.412E+00	8.269E-02
27.25	1.420E+00	7.9	29.45	1.230E+00	9.767E-02
27.75	1.713E+00	5.8	29.99	1.485E+00	8.655E-02
28.45	1.474E+00	8.8	30.74	1.279E+00	1.129E-01
28.75	1.655E+00	9.6	31.07	1.437E+00	1.380E-01
29.34	1.339E+00	6.8	31.70	1.163E+00	7.873E-02
29.95	1.160E+00	8.5	32.35	1.009E+00	8.603E-02
30.25	1.168E+00	6.8	32.67	1.016E+00	6.948E-02
30.95	1.321E+00	4.9	33.43	1.150E+00	5.611E-02
31.45	1.232E+00	8.1	33.96	1.074E+00	8.682E-02
31.75	9.931E-01	10.7	34.28	8.659E-01	9.307E-02
32.45	1.378E+00	8.0	35.03	1.203E+00	9.614E-02
32.84	1.120E+00	8.1	35.45	9.777E-01	7.890E-02
33.25	9.887E-01	6.7	35.89	8.640E-01	5.806E-02



SCATTERING OF 4-HE PARTICLES ON TI-50

ELAB = 104.000 MEV    Q = -4.420 MEV    I = 3 -  
 ECM = 91.871 MEV    K = 4.0363/FERMI    ETA = 1.39171

LABORATORY DATA			CM DATA		
THETA DEGREE	SIGMA MB/SR	DSIGMA %	THETA DEGREE	SIGMA MB/SR	DSIGMA MB/SR
7.45	3.599E+01	23.5	8.07	3.067E+01	7.207E+00
8.95	2.975E+01	19.2	9.70	2.537E+01	4.876E+00
9.34	2.886E+01	9.4	10.12	2.461E+01	2.306E+00
9.84	2.315E+01	5.7	10.66	1.975E+01	1.135E+00
10.34	1.701E+01	10.5	11.20	1.451E+01	1.520E+00
10.75	8.728E+00	22.5	11.65	7.449E+00	1.673E+00
10.95	1.058E+01	13.1	11.86	9.031E+00	1.185E+00
11.25	8.194E+00	15.5	12.19	6.918E+00	1.073E+00
11.45	7.281E+00	12.9	12.41	6.216E+00	7.994E-01
11.75	9.321E+00	20.7	12.73	7.959E+00	1.651E+00
11.95	5.748E+00	37.2	12.95	4.909E+00	1.828E+00
12.25	9.241E+00	15.3	13.27	7.893E+00	1.205E+00
12.45	8.390E+00	11.8	13.49	7.167E+00	8.474E-01
12.75	1.047E+01	11.7	13.81	8.947E+00	1.046E+00
12.95	9.053E+00	10.6	14.03	7.736E+00	8.174E-01
13.25	7.791E+00	10.3	14.35	6.659E+00	6.831E-01
13.45	8.667E+00	10.1	14.57	7.408E+00	7.509E-01
13.75	1.030E+01	9.3	14.89	8.805E+00	8.155E-01
13.95	8.977E+00	15.3	15.11	7.676E+00	1.171E+00
14.25	5.559E+00	21.7	15.43	4.754E+00	1.031E+00
14.45	6.499E+00	10.5	15.65	5.559E+00	5.835E-01
14.75	5.780E+00	13.9	15.98	4.945E+00	6.892E-01
14.95	7.303E+00	11.5	16.19	6.249E+00	7.193E-01
15.29	6.309E+00	7.4	16.56	5.400E+00	3.982E-01
15.81	7.111E+00	5.0	17.13	6.089E+00	3.034E-01
16.33	5.933E+00	10.0	17.69	5.082E+00	5.066E-01
16.75	6.461E+00	18.5	18.14	5.536E+00	1.024E+00
16.95	5.087E+00	18.6	18.35	4.360E+00	8.093E-01
17.25	4.983E+00	23.4	18.68	4.272E+00	9.998E-01
17.45	3.499E+00	26.1	18.89	3.000E+00	7.833E-01
17.75	3.352E+00	26.7	19.22	2.875E+00	7.685E-01
17.95	2.479E+00	22.9	19.43	2.126E+00	4.864E-01
18.25	2.267E+00	22.0	19.76	1.945E+00	4.280E-01
18.45	1.985E+00	33.9	19.97	1.703E+00	5.777E-01
18.75	1.998E+00	19.2	20.30	1.715E+00	3.295E-01
18.95	1.974E+00	18.0	20.51	1.695E+00	3.056E-01
19.25	2.206E+00	15.2	20.84	1.894E+00	2.871E-01
19.45	2.330E+00	16.2	21.05	2.001E+00	3.247E-01
19.95	2.885E+00	11.9	21.59	2.479E+00	2.952E-01
20.45	3.933E+00	9.0	22.13	3.381E+00	3.026E-01
20.95	4.630E+00	6.2	22.67	3.983E+00	2.484E-01
22.34	3.872E+00	4.2	24.17	3.335E+00	1.392E-01
23.95	1.789E+00	9.8	25.90	1.544E+00	1.520E-01
25.45	1.246E+00	10.5	27.52	1.077E+00	1.130E-01
26.25	1.334E+00	8.3	28.38	1.154E+00	9.601E-02
26.90	1.630E+00	5.9	29.08	1.412E+00	8.269E-02
27.25	1.420E+00	7.9	29.45	1.230E+00	9.767E-02
27.75	1.713E+00	5.8	29.99	1.485E+00	9.655E-02
28.45	1.474E+00	8.8	30.74	1.279E+00	1.129E-01
28.75	1.655E+00	9.6	31.07	1.437E+00	1.380E-01
29.34	1.339E+00	6.8	31.70	1.163E+00	7.873E-02
29.95	1.160E+00	8.5	32.35	1.009E+00	8.603E-02
30.25	1.168E+00	6.8	32.67	1.016E+00	6.948E-02
30.95	1.321E+00	4.9	33.43	1.150E+00	5.611E-02
31.45	1.232E+00	8.1	33.96	1.074E+00	8.682E-02
31.75	9.931E-01	10.7	34.28	8.659E-01	9.307E-02
32.45	1.378E+00	8.0	35.03	1.203E+00	9.614E-02
32.84	1.120E+00	8.1	35.45	9.777E-01	7.890E-02
33.25	9.887E-01	6.7	35.89	8.640E-01	5.806E-02

33.95	7.784E-01	9.4	36.64	6.810E-01	6.408E-02
34.45	1.023E+00	10.4	37.17	8.961E-01	9.327E-02
34.75	7.695E-01	9.9	37.49	6.741E-01	6.664E-02
35.25	7.946E-01	5.6	38.03	6.966E-01	3.931E-02
35.95	9.045E-01	7.1	38.78	7.939E-01	5.660E-02
36.34	7.439E-01	5.7	39.19	6.534E-01	3.726E-02
36.75	7.534E-01	6.4	39.63	6.622E-01	4.211E-02
37.45	8.839E-01	5.9	40.38	7.778E-01	4.558E-02
37.95	7.897E-01	4.5	40.91	6.955E-01	3.158E-02
38.25	7.484E-01	5.9	41.23	6.595E-01	3.871E-02
38.75	6.526E-01	5.4	41.76	5.756E-01	3.102E-02
39.45	5.227E-01	5.7	42.51	4.616E-01	2.639E-02
39.84	5.281E-01	2.5	42.92	4.667E-01	1.168E-02
40.25	5.233E-01	4.3	43.36	4.628E-01	2.004E-02
41.45	4.710E-01	2.9	44.64	4.175E-01	1.212E-02
41.75	4.535E-01	5.9	44.96	4.022E-01	2.364E-02
42.25	3.579E-01	6.0	45.49	3.177E-01	1.921E-02
42.95	4.142E-01	4.3	46.23	3.682E-01	1.566E-02
43.34	3.770E-01	14.3	46.64	3.354E-01	4.807E-02
43.75	4.316E-01	4.5	47.08	3.843E-01	1.748E-02
44.45	3.657E-01	3.4	47.82	3.260E-01	1.098E-02
44.95	3.680E-01	13.3	48.35	3.284E-01	4.370E-02
45.25	3.081E-01	7.4	48.67	2.751E-01	2.032E-02
45.75	2.598E-01	16.1	49.20	2.322E-01	3.738E-02
46.45	3.027E-01	17.0	49.94	2.710E-01	4.597E-02
46.84	2.813E-01	3.8	50.35	2.520E-01	9.524E-03
47.25	2.854E-01	15.6	50.78	2.559E-01	3.988E-02
47.95	2.327E-01	17.1	51.52	2.090E-01	3.578E-02
48.45	2.449E-01	4.7	52.05	2.202E-01	1.038E-02
48.75	2.690E-01	14.7	52.37	2.420E-01	3.546E-02
49.25	1.953E-01	7.4	52.90	1.759E-01	1.307E-02
49.95	2.165E-01	6.0	53.63	1.953E-01	1.175E-02
50.78	2.836E-01	4.7	54.51	2.562E-01	1.197E-02
51.41	2.445E-01	3.4	55.17	2.212E-01	7.555E-03
51.84	2.488E-01	5.5	55.62	2.253E-01	1.233E-02
52.25	2.282E-01	5.0	56.06	2.069E-01	1.036E-02
52.45	2.431E-01	8.5	56.27	2.205E-01	1.871E-02
52.95	1.742E-01	12.0	56.79	1.582E-01	1.893E-02
53.45	2.394E-01	7.5	57.32	2.176E-01	1.628E-02
53.95	2.099E-01	7.9	57.84	1.910E-01	1.506E-02
54.45	2.282E-01	7.1	58.37	2.079E-01	1.481E-02
54.95	1.824E-01	10.9	58.89	1.664E-01	1.814E-02
55.45	1.750E-01	7.1	59.41	1.598E-01	1.140E-02
55.95	1.683E-01	5.3	59.94	1.539E-01	8.232E-03
56.39	1.685E-01	6.6	60.40	1.542E-01	1.019E-02
56.84	1.615E-01	7.1	60.87	1.480E-01	1.058E-02
57.34	1.635E-01	7.1	61.39	1.500E-01	1.065E-02
57.95	1.365E-01	7.3	62.03	1.254E-01	9.204E-03
58.45	1.457E-01	6.9	62.55	1.340E-01	9.206E-03
58.95	1.529E-01	7.1	63.07	1.408E-01	1.002E-02
59.45	1.247E-01	9.6	63.59	1.150E-01	1.104E-02
59.95	1.075E-01	10.7	64.12	9.928E-02	1.066E-02
60.45	1.249E-01	10.1	64.64	1.155E-01	1.172E-02
60.95	9.135E-02	10.6	65.16	8.456E-02	8.955E-03
61.45	1.002E-01	8.7	65.68	9.284E-02	8.052E-03
61.95	1.150E-01	7.9	66.20	1.067E-01	8.467E-03
63.34	8.156E-02	7.7	67.64	7.596E-02	5.811E-03
64.95	8.101E-02	7.1	69.31	7.576E-02	5.368E-03
66.45	6.206E-02	10.3	70.86	5.827E-02	6.001E-03
67.95	6.595E-02	7.5	72.41	6.217E-02	4.634E-03
69.34	5.198E-02	9.8	73.84	4.918E-02	4.803E-03
70.95	4.788E-02	8.8	75.50	4.550E-02	4.025E-03
72.45	3.305E-02	13.4	77.04	3.154E-02	4.228E-03
73.95	2.722E-02	12.3	78.57	2.609E-02	3.222E-03
76.95	1.457E-02	18.7	81.64	1.408E-02	2.630E-03
78.45	1.470E-02	22.5	83.16	1.427E-02	3.209E-03
79.95	9.292E-03	25.0	84.69	9.057E-03	2.261E-03
84.45	4.875E-03	38.5	89.24	4.765E-03	1.837E-03
85.95	1.949E-03	77.6	90.75	1.933E-03	1.499E-03

SCATTERING OF 4-HE PARTICLES ON TI-50

ELAB = 104.000 MEV    Q = -2.695 MEV    I = 4 +  
 ECM = 93.596 MEV    K = 4.0740/FERMI    ETA = 1.37882

LABORATORY DATA			CM DATA		
THETA DEGREE	SIGMA MB/SR	DSIGMA %	THETA DEGREE	SIGMA MB/SR	DSIGMA MB/SR
8.95	6.378E+00	11.4	9.69	5.446E+00	6.187E-01
9.34	7.029E+00	11.9	10.11	6.003E+00	7.139E-01
9.65	5.535E+00	16.5	10.45	4.728E+00	7.821E-01
9.84	6.847E+00	12.6	10.66	5.849E+00	7.358E-01
10.34	5.929E+00	10.0	11.20	5.066E+00	5.060E-01
10.67	5.453E+00	10.9	11.55	4.660E+00	5.090E-01
10.95	5.396E+00	12.7	11.86	4.612E+00	5.856E-01
11.17	4.651E+00	11.4	12.09	3.976E+00	4.536E-01
11.45	4.674E+00	15.5	12.40	3.996E+00	6.199E-01
11.68	3.495E+00	18.4	12.64	2.988E+00	5.486E-01
11.95	2.969E+00	10.8	12.94	2.539E+00	2.752E-01
12.17	3.052E+00	13.1	13.18	2.610E+00	3.410E-01
12.45	2.677E+00	23.5	13.48	2.290E+00	5.378E-01
12.68	1.922E+00	19.8	13.73	1.644E+00	3.250E-01
12.95	1.803E+00	31.4	14.02	1.543E+00	4.846E-01
13.19	1.458E+00	19.3	14.27	1.248E+00	2.404E-01
13.45	1.157E+00	33.2	14.56	9.902E-01	3.284E-01
13.69	9.610E-01	20.0	14.82	8.227E-01	1.648E-01
13.95	6.408E-01	37.6	15.10	5.487E-01	2.061E-01
14.21	5.170E-01	26.1	15.38	4.427E-01	1.158E-01
14.68	5.513E-01	21.9	15.89	4.723E-01	1.037E-01
14.95	6.326E-01	31.2	16.18	5.420E-01	1.693E-01
15.15	8.162E-01	23.1	16.40	6.994E-01	1.613E-01
15.66	1.231E+00	23.8	16.95	1.055E+00	2.506E-01
16.15	1.378E+00	12.2	17.48	1.182E+00	1.439E-01
16.34	1.300E+00	20.1	17.68	1.115E+00	2.247E-01
16.66	1.564E+00	20.5	18.02	1.342E+00	2.755E-01
17.15	1.594E+00	18.9	18.56	1.368E+00	2.572E-01
17.45	1.641E+00	19.3	18.88	1.409E+00	2.718E-01
17.66	1.548E+00	18.7	19.11	1.329E+00	2.485E-01
17.95	1.542E+00	15.8	19.42	1.324E+00	2.095E-01
18.18	1.473E+00	10.2	19.67	1.265E+00	1.286E-01
18.45	1.260E+00	37.1	19.96	1.083E+00	4.021E-01
18.68	1.208E+00	13.6	20.20	1.038E+00	1.413E-01
18.95	1.003E+00	26.4	20.50	8.626E-01	2.275E-01
19.18	8.930E-01	18.6	20.74	7.678E-01	1.428E-01
19.45	6.939E-01	38.2	21.04	5.968E-01	2.283E-01
19.65	4.792E-01	29.8	21.25	4.122E-01	1.226E-01
19.95	4.273E-01	42.6	21.58	3.677E-01	1.566E-01
20.15	3.254E-01	32.5	21.79	2.800E-01	9.095E-02
20.45	3.330E-01	62.5	22.12	2.867E-01	1.791E-01
20.65	1.823E-01	55.0	22.33	1.570E-01	8.627E-02
20.95	2.323E-01	63.8	22.66	2.001E-01	1.277E-01
21.65	5.783E-01	24.7	23.41	4.984E-01	1.232E-01
22.15	7.333E-01	18.6	23.95	6.324E-01	1.175E-01
22.34	7.559E-01	9.7	24.15	6.520E-01	6.304E-02
22.65	7.582E-01	15.8	24.49	6.542E-01	1.035E-01
23.15	7.675E-01	13.9	25.03	6.626E-01	9.235E-02
23.65	7.866E-01	17.7	25.56	6.794E-01	1.199E-01
23.95	6.058E-01	12.3	25.89	5.234E-01	6.418E-02
24.15	5.993E-01	18.2	26.10	5.179E-01	9.443E-02
24.65	6.250E-01	15.5	26.64	5.405E-01	8.370E-02
25.15	5.250E-01	18.8	27.18	4.543E-01	9.557E-02
25.45	3.585E-01	21.4	27.50	3.103E-01	6.639E-02
26.21	2.836E-01	19.0	28.32	2.457E-01	4.675E-02
26.65	1.953E-01	29.9	28.79	1.693E-01	5.067E-02
26.84	1.945E-01	18.7	28.99	1.686E-01	3.159E-02
27.15	1.883E-01	37.7	29.33	1.633E-01	6.162E-02
27.65	8.594E-02	66.2	29.86	7.459E-02	4.936E-02
28.15	1.855E-01	29.0	30.40	1.611E-01	4.671E-02
28.45	2.048E-01	19.0	30.72	1.779E-01	3.386E-02
28.69	2.349E-01	33.0	30.98	2.042E-01	6.744E-02
29.10	2.696E-01	15.2	31.42	2.345E-01	3.566E-02
29.34	2.671E-01	11.6	31.68	2.324E-01	2.692E-02
29.95	2.674E-01	23.6	32.33	2.328E-01	5.495E-02
30.10	3.514E-01	18.2	32.49	3.060E-01	5.575E-02
30.25	3.178E-01	13.3	32.65	2.768E-01	3.683E-02
30.95	3.300E-01	8.4	33.40	2.877E-01	2.419E-02
31.45	3.072E-01	12.9	33.94	2.680E-01	3.463E-02
31.75	2.721E-01	9.9	34.26	2.375E-01	2.344E-02

32.10	2.877E-01	13.3	34.63	2.513E-01	3.339E-02
32.45	2.518E-01	12.3	35.01	2.200E-01	2.706E-02
32.84	2.370E-01	10.7	35.43	2.072E-01	2.223E-02
33.10	2.106E-01	15.6	35.71	1.842E-01	2.874E-02
33.25	2.080E-01	15.6	35.86	1.820E-01	2.839E-02
34.10	1.952E-01	16.1	36.77	1.710E-01	2.747E-02
35.10	1.541E-01	13.1	37.84	1.352E-01	1.775E-02
35.95	1.339E-01	20.5	38.75	1.177E-01	2.408E-02
36.10	1.510E-01	15.9	38.91	1.327E-01	2.116E-02
36.34	1.426E-01	9.7	39.17	1.254E-01	1.216E-02
36.75	1.474E-01	21.9	39.60	1.297E-01	2.836E-02
37.10	1.695E-01	12.7	39.98	1.492E-01	1.893E-02
37.45	1.381E-01	16.9	40.35	1.217E-01	2.062E-02
37.95	1.324E-01	12.8	40.88	1.167E-01	1.500E-02
38.10	1.510E-01	19.0	41.04	1.332E-01	2.531E-02
38.25	1.233E-01	19.1	41.20	1.088E-01	2.083E-02
38.75	1.132E-01	12.3	41.74	9.995E-02	1.225E-02
39.10	1.259E-01	14.7	42.11	1.112E-01	1.635E-02
39.45	1.209E-01	12.3	42.48	1.069E-01	1.320E-02
39.84	1.114E-01	5.6	42.90	9.855E-02	5.472E-03
40.10	1.105E-01	30.3	43.17	9.780E-02	2.963E-02
40.25	1.139E-01	13.7	43.33	1.008E-01	1.383E-02
41.10	1.130E-01	13.6	44.24	1.002E-01	1.368E-02
41.45	1.103E-01	6.1	44.61	9.787E-02	5.994E-03
41.75	1.102E-01	9.2	44.93	9.787E-02	9.034E-03
42.10	1.156E-01	14.3	45.30	1.027E-01	1.471E-02
42.25	1.051E-01	7.3	45.46	9.339E-02	6.780E-03
42.95	1.032E-01	8.0	46.20	9.184E-02	7.375E-03
43.10	1.113E-01	16.4	46.36	9.907E-02	1.624E-02
43.34	1.030E-01	25.7	46.61	9.171E-02	2.356E-02
43.75	1.013E-01	8.3	47.05	9.024E-02	7.465E-03
44.45	8.223E-02	7.6	47.79	7.338E-02	5.576E-03
44.95	7.428E-02	33.8	48.32	6.636E-02	2.245E-02
45.10	8.220E-02	27.4	48.48	7.345E-02	2.013E-02
45.25	7.170E-02	10.5	48.64	6.409E-02	6.752E-03
45.75	6.615E-02	38.1	49.17	5.919E-02	2.257E-02
46.45	7.011E-02	41.1	49.91	6.282E-02	2.584E-02
46.84	6.878E-02	7.9	50.32	6.168E-02	4.890E-03
47.25	6.378E-02	53.9	50.75	5.724E-02	3.083E-02
47.95	6.484E-02	33.6	51.49	5.828E-02	1.958E-02
48.45	6.315E-02	7.9	52.02	5.682E-02	4.466E-03
48.75	6.504E-02	32.2	52.34	5.856E-02	1.884E-02
49.25	5.923E-02	7.4	52.86	5.339E-02	3.951E-03
49.95	5.518E-02	12.9	53.60	4.981E-02	6.423E-03
50.79	5.346E-02	10.2	54.49	4.835E-02	4.920E-03
51.40	5.697E-02	6.5	55.13	5.159E-02	3.377E-03
51.84	5.430E-02	13.2	55.59	4.922E-02	6.488E-03
52.25	5.417E-02	7.4	56.02	4.915E-02	3.631E-03
52.45	5.278E-02	14.3	56.23	4.791E-02	6.849E-03
52.95	5.384E-02	8.9	56.76	4.893E-02	4.298E-03
53.45	5.561E-02	11.5	57.28	5.059E-02	5.820E-03
53.95	4.835E-02	17.4	57.81	4.404E-02	7.663E-03
54.45	4.428E-02	12.6	58.33	4.038E-02	5.107E-03
54.95	3.983E-02	22.6	58.85	3.636E-02	8.229E-03
55.45	3.952E-02	14.7	59.38	3.612E-02	5.316E-03
55.95	3.712E-02	12.0	59.90	3.397E-02	4.089E-03
56.39	4.162E-02	9.9	60.37	3.812E-02	3.756E-03
56.84	4.107E-02	14.7	60.83	3.766E-02	5.553E-03
57.34	4.263E-02	14.0	61.35	3.914E-02	5.499E-03
57.95	4.319E-02	12.4	61.99	3.971E-02	4.928E-03
58.45	3.897E-02	12.8	62.51	3.587E-02	4.583E-03
58.95	3.843E-02	13.3	63.04	3.542E-02	4.705E-03
59.45	3.427E-02	18.2	63.56	3.162E-02	5.758E-03
59.95	2.753E-02	21.6	64.08	2.544E-02	5.496E-03
60.45	2.257E-02	27.9	64.60	2.088E-02	5.920E-03
60.95	2.538E-02	18.0	65.12	2.351E-02	4.229E-03
61.45	2.722E-02	16.3	65.64	2.524E-02	4.122E-03
61.95	2.489E-02	18.5	66.16	2.311E-02	4.283E-03
63.34	2.304E-02	14.2	67.60	2.147E-02	3.054E-03
64.95	1.229E-02	21.8	69.27	1.150E-02	2.508E-03
66.45	1.004E-02	37.3	70.82	9.429E-03	3.519E-03
67.95	9.601E-03	22.7	72.37	9.055E-03	2.060E-03
69.34	7.650E-03	35.9	73.80	7.242E-03	2.598E-03
70.95	6.101E-03	34.5	75.46	5.801E-03	2.004E-03
72.45	4.819E-03	42.6	77.00	4.601E-03	1.961E-03
73.95	3.354E-03	39.3	78.53	3.215E-03	1.262E-03
76.95	3.565E-03	48.3	81.59	3.446E-03	1.663E-03
78.45	3.267E-03	84.0	83.12	3.172E-03	2.663E-03
79.95	3.958E-03	37.5	84.64	3.859E-03	1.446E-03
85.95	2.219E-03	72.4	90.70	2.201E-03	1.593E-03

SCATTERING OF 4-HE PARTICLES ON CR-52

ELAB = 104.000 MEV    Q = 0.0 MEV    I = 0 +  
 ECM = 96.559 MEV    K = 4.1437/FERMI    ETA = 1.48297

LABORATORY DATA			RUTHERFORD	CM DATA		
THETA DEGREE	SIGMA MB/SR	DSIGMA %	SIGMA/SR	THETA DEGREE	SIGMA MB/SR	DSIGMA MB/SR
2.34	1.259F+06	78.4	7.955E-01	2.52	1.081E+06	8.472E+05
2.84	5.305E+05	99.6	7.275E-01	3.06	4.557E+05	4.540E+05
3.34	2.527E+05	20.3	6.629E-01	3.60	2.171E+05	4.414E+04
3.88	1.460E+05	20.5	6.949E-01	4.18	1.254E+05	2.573E+04
4.35	8.722E+04	30.9	6.574E-01	4.69	7.494E+04	2.317E+04
4.95	5.011E+04	12.5	6.337E-01	5.34	4.306E+04	5.367E+03
5.45	3.326E+04	15.8	6.178E-01	5.88	2.858E+04	4.510E+03
5.95	1.766E+04	34.7	4.660E-01	6.42	1.518E+04	5.264E+03
6.45	9.077E+03	24.4	3.306E-01	6.96	7.803E+03	1.906E+03
6.95	3.818E+03	20.0	1.874E-01	7.50	3.283E+03	6.574E+02
7.45	1.978E+03	19.7	1.281E-01	8.04	1.701E+03	3.347E+02
7.95	1.415E+03	10.2	1.188E-01	8.58	1.217E+03	1.242E+02
8.95	1.987E+03	6.9	2.678E-01	9.65	1.710E+03	1.188E+02
9.34	2.421E+03	7.2	3.867E-01	10.08	2.083E+03	1.497E+02
10.34	2.031E+03	7.8	4.871E-01	11.15	1.749E+03	1.370E+02
10.75	1.633E+03	11.4	4.571E-01	11.59	1.406E+03	1.603E+02
10.95	1.433E+03	16.2	4.318E-01	11.81	1.234E+03	2.003E+02
11.25	1.178E+03	28.6	3.955E-01	12.13	1.015E+03	2.898E+02
11.45	6.271E+02	39.5	2.258E-01	12.35	5.402E+02	2.132E+02
11.75	7.271E+02	12.2	2.903E-01	12.67	6.265E+02	7.626E+01
11.95	5.727E+02	23.5	2.445E-01	12.89	4.935E+02	1.162E+02
12.25	2.990E+02	43.7	1.409E-01	13.21	2.577E+02	1.126E+02
12.45	1.549E+02	48.0	7.786E-02	13.43	1.335E+02	6.408E+01
12.75	9.249E+01	32.4	5.112E-02	13.75	7.973E+01	2.580E+01
12.95	5.933E+01	43.4	3.489E-02	13.97	5.115E+01	2.222E+01
13.25	7.416E+00	140.5	4.778E-03	14.29	6.395E+00	8.982E+00
13.45	6.188E+00	135.9	4.232E-03	14.50	5.337E+00	7.251E+00
13.75	3.368E+01	50.5	2.514E-02	14.83	2.905E+01	1.466E+01
13.95	5.930E+01	40.6	4.689E-02	15.04	5.116E+01	2.076E+01
14.25	1.110E+02	18.0	9.552E-02	15.36	9.576E+01	1.719E+01
14.45	9.567E+01	36.4	8.703E-02	15.58	8.256E+01	3.004E+01
14.75	2.032E+02	21.7	2.006E-01	15.90	1.754E+02	3.809E+01
14.95	1.646E+02	16.8	1.714E-01	16.12	1.421E+02	2.392E+01
15.29	2.171E+02	8.7	2.475E-01	16.49	1.875E+02	1.631E+01
15.78	2.571E+02	2.9	3.317E-01	17.01	2.221E+02	6.535E+00
16.30	2.512E+02	4.4	3.689E-01	17.57	2.171E+02	9.636E+00
16.75	1.937E+02	8.7	3.169E-01	18.06	1.674E+02	1.456E+01
16.95	1.772E+02	8.8	3.040E-01	18.27	1.532E+02	1.344E+01
17.25	1.436E+02	10.7	2.642E-01	18.59	1.242E+02	1.329E+01
17.45	1.276E+02	8.6	2.458E-01	18.81	1.104E+02	9.471E+00
17.75	1.107E+02	16.0	2.280E-01	19.13	9.576E+01	1.532E+01
17.95	7.780E+01	21.0	1.676E-01	19.35	6.732E+01	1.414E+01
18.25	6.593E+01	27.8	1.517E-01	19.67	5.706E+01	1.588E+01
18.45	2.803E+01	55.5	6.731E-02	19.88	2.426E+01	1.346E+01
18.75	2.661E+01	21.6	6.813E-02	20.21	2.304E+01	4.980E+00
18.95	1.320E+01	45.1	3.525E-02	20.42	1.143E+01	5.150E+00
19.25	1.535E+01	28.7	4.363E-02	20.74	1.330E+01	3.812E+00
19.45	5.820E+00	110.9	1.723E-02	20.96	5.042E+00	5.591E+00
19.75	1.570E+01	31.2	4.940E-02	21.28	1.361E+01	4.251E+00
19.95	1.117E+01	33.4	3.656E-02	21.50	9.680E+00	3.228E+00
20.45	2.308E+01	18.1	8.332E-02	22.03	2.001E+01	3.628E+00
20.95	3.721E+01	11.1	1.478E-01	22.57	3.228E+01	3.584E+00
21.34	4.624E+01	6.2	1.976E-01	22.99	4.013E+01	2.490E+00
21.75	5.141E+01	2.1	2.369E-01	23.43	4.464E+01	9.262E-01
22.34	5.172E+01	1.3	2.649E-01	24.06	4.493E+01	5.702E-01
22.95	4.742E+01	10.5	2.701E-01	24.72	4.122E+01	4.320E+00
23.25	4.056E+01	12.0	2.432E-01	25.04	3.527E+01	4.218E+00
23.95	2.796E+01	8.0	1.884E-01	25.79	2.433E+01	1.958E+00
24.45	1.854E+01	12.5	1.355E-01	26.32	1.614E+01	2.013E+00
24.75	1.553E+01	19.1	1.192E-01	26.65	1.353E+01	1.369E+00
25.45	8.804E+00	10.5	7.537E-02	27.40	7.674E+00	8.090E-01
25.95	7.851E+00	5.8	7.255E-02	27.93	6.847E+00	3.940E-01
26.25	7.933E+00	5.8	7.670E-02	28.25	6.921E+00	4.008E-01
26.87	1.029E+01	7.3	1.091E-01	28.92	8.984E+00	6.568E-01
27.25	1.179E+01	10.8	1.320E-01	29.32	1.030E+01	1.110E+00
27.75	1.367E+01	7.9	1.644E-01	29.86	1.195E+01	9.463E-01
28.45	1.456E+01	3.4	1.931E-01	30.61	1.274E+01	4.340E-01
28.75	1.416E+01	1.8	1.956E-01	30.93	1.239E+01	2.229E-01
29.34	1.313E+01	4.1	1.964E-01	31.56	1.150E+01	4.719E-01

29.95	1.013E+01	11.2	1.642E-01	32.21	8.880E+00	9.962E-01
30.25	9.807E+00	14.8	1.653E-01	32.53	8.600E+00	1.276E+00
30.95	6.724E+00	14.5	1.239E-01	33.28	5.902E+00	8.562E-01
31.45	5.221E+00	17.6	1.024E-01	33.81	4.586E+00	8.093E-01
31.75	4.413E+00	17.8	8.985E-02	34.13	3.878E+00	6.891E-01
32.45	3.222E+00	5.2	7.141E-02	34.88	2.834E+00	1.469E-01
32.84	3.216E+00	1.4	7.467E-02	35.30	2.830E+00	3.998E-02
33.25	3.095E+00	1.4	7.543E-02	35.73	2.726E+00	3.775E-02
33.95	3.179E+00	3.2	8.398E-02	36.48	2.802E+00	8.838E-02
34.45	3.704E+00	7.8	1.036E-01	37.01	3.268E+00	2.559E-01
34.75	3.643E+00	7.1	1.053E-01	37.33	3.215E+00	2.293E-01
35.25	3.618E+00	3.9	1.106E-01	37.86	3.196E+00	1.246E-01
35.95	3.351E+00	6.9	1.105E-01	38.61	2.963E+00	2.053E-01
36.34	3.031E+00	6.2	1.042E-01	39.02	2.682E+00	1.655E-01
36.75	2.437E+00	5.1	8.754E-02	39.46	2.158E+00	1.101E-01
37.45	1.966E+00	7.0	7.596E-02	40.20	1.743E+00	1.216E-01
37.95	1.463E+00	11.3	5.948E-02	40.74	1.298E+00	1.461E-01
38.25	1.537E+00	9.7	6.440E-02	41.05	1.364E+00	1.320E-01
38.75	1.317E+00	7.5	5.802E-02	41.59	1.170E+00	8.830E-02
39.45	1.061E+00	5.3	5.005E-02	42.33	9.432E-01	4.977E-02
39.84	1.129E+00	3.2	5.534E-02	42.74	1.005E+00	3.249E-02
40.25	1.036E+00	3.5	5.279E-02	43.18	9.224E-01	3.204E-02
40.95	1.167E+00	3.1	6.357E-02	43.92	1.041E+00	3.274E-02
41.45	1.271E+00	7.7	7.248E-02	44.45	1.134E+00	8.711E-02
41.75	1.308E+00	10.1	7.670E-02	44.77	1.168E+00	1.175E-01
42.25	1.276E+00	4.3	7.828E-02	45.30	1.140E+00	4.886E-02
42.95	1.228E+00	1.7	8.024E-02	46.04	1.099E+00	1.868E-02
43.34	1.204E+00	2.2	8.140E-02	46.45	1.078E+00	2.412E-02
43.75	1.120E+00	2.8	7.852E-02	46.88	1.004E+00	2.824E-02
44.45	1.008E+00	2.1	7.507E-02	47.62	9.048E-01	1.913E-02
44.95	9.931E-01	6.7	7.714E-02	48.15	8.920E-01	5.972E-02
45.25	8.955E-01	9.0	7.134E-02	48.47	8.048E-01	7.225E-02
45.75	8.482E-01	5.0	7.044E-02	48.99	7.630E-01	3.802E-02
46.45	8.874E-01	5.2	7.806E-02	49.73	7.994E-01	4.141E-02
46.84	7.843E-01	5.7	7.120E-02	50.14	7.070E-01	4.040E-02
47.25	9.009E-01	3.1	8.452E-02	50.58	8.128E-01	2.492E-02
47.95	8.758E-01	2.4	8.685E-02	51.31	7.913E-01	1.936E-02
48.45	7.869E-01	12.1	8.114E-02	51.84	7.117E-01	8.615E-02
48.75	8.249E-01	12.7	8.705E-02	52.16	7.465E-01	9.502E-02
49.25	8.172E-01	5.8	8.961E-02	52.68	7.403E-01	4.330E-02
49.95	7.287E-01	4.1	8.425E-02	53.42	6.611E-01	2.690E-02
50.79	7.010E-01	1.5	8.625E-02	54.30	6.370E-01	9.686E-03
51.43	6.451E-01	2.3	8.318E-02	54.97	5.870E-01	1.327E-02
51.84	6.693E-01	5.1	8.889E-02	55.40	6.096E-01	3.104E-02
52.25	6.178E-01	16.2	8.450E-02	55.83	5.632E-01	9.125E-02
52.45	6.003E-01	12.5	8.327E-02	56.04	5.474E-01	6.861E-02
52.95	5.924E-01	2.6	8.512E-02	56.56	5.408E-01	1.432E-02
53.45	5.512E-01	3.7	8.203E-02	57.09	5.038E-01	1.850E-02
53.95	4.938E-01	2.2	7.606E-02	57.61	4.518E-01	1.011E-02
54.45	4.927E-01	2.9	7.852E-02	58.13	4.513E-01	1.328E-02
54.95	4.619E-01	3.4	7.613E-02	58.66	4.235E-01	1.421E-02
55.45	4.377E-01	1.5	7.460E-02	59.18	4.018E-01	5.889E-03
55.95	4.385E-01	2.7	7.726E-02	59.70	4.030E-01	1.074E-02
56.40	4.293E-01	2.1	7.788E-02	60.17	3.949E-01	8.446E-03
56.84	4.458E-01	2.5	8.322E-02	60.63	4.105E-01	1.046E-02
57.34	4.306E-01	3.4	8.302E-02	61.15	3.970E-01	1.341E-02
57.95	3.996E-01	3.1	8.007E-02	61.79	3.689E-01	1.137E-02
58.45	3.815E-01	3.0	7.889E-02	62.31	3.526E-01	1.051E-02
58.95	3.535E-01	5.3	7.540E-02	62.83	3.271E-01	1.730E-02
59.45	2.871E-01	6.0	6.316E-02	63.35	2.660E-01	1.596E-02
59.95	2.636E-01	4.1	5.978E-02	63.87	2.445E-01	1.001E-02
60.45	2.702E-01	4.7	6.314E-02	64.39	2.509E-01	1.182E-02
60.95	2.657E-01	3.9	6.397E-02	64.91	2.470E-01	9.653E-03
61.45	2.490E-01	3.5	6.176E-02	65.43	2.318E-01	8.041E-03
61.95	2.333E-01	4.3	5.957E-02	65.95	2.174E-01	9.318E-03
63.34	1.958E-01	3.8	5.416E-02	67.39	1.831E-01	6.930E-03
64.95	1.575E-01	4.3	4.763E-02	69.05	1.478E-01	6.347E-03
66.45	1.247E-01	4.6	4.092E-02	70.60	1.175E-01	5.400E-03
67.95	9.711E-02	4.5	3.448E-02	72.15	9.184E-02	4.098E-03
69.34	8.665E-02	7.0	3.303E-02	73.58	8.224E-02	5.752E-03
70.95	6.877E-02	7.8	2.841E-02	75.23	6.554E-02	5.144E-03
72.45	5.052E-02	9.1	2.244E-02	76.77	4.834E-02	4.419E-03
73.95	4.054E-02	9.3	1.932E-02	78.30	3.894E-02	3.622E-03
75.34	3.727E-02	7.5	1.893E-02	79.72	3.593E-02	2.690E-03
76.95	2.490E-02	9.8	1.359E-02	81.36	2.411E-02	2.366E-03
78.45	1.981E-02	10.8	1.154E-02	82.89	1.926E-02	2.074E-03
79.95	1.663E-02	10.3	1.032E-02	84.41	1.623E-02	1.679E-03
81.34	1.159E-02	13.9	7.622E-03	85.81	1.136E-02	1.584E-03
82.95	1.059E-02	13.3	7.425E-03	87.44	1.042E-02	1.384E-03
84.45	7.204E-03	17.6	5.357E-03	88.95	7.118E-03	1.250E-03
85.95	5.854E-03	17.6	4.608E-03	90.46	5.808E-03	1.022E-03

SCATTERING OF 4-HE PARTICLES ON CR-52

ELAB = 104.000 MEV    Q = -1.434 MEV    I = 2 +  
 ECM = 95.125 MEV    K = 4.1129/FERMI    ETA = 1.49411

LABORATORY DATA			CM DATA		
THETA DEGREE	SIGMA MB/SR	DSIGMA %	THETA DEGREE	SIGMA MB/SR	DSIGMA MB/SR
11.95	2.024E+01	5.7	12.89	1.742E+01	1.000E+00
12.25	2.186E+01	5.2	13.22	1.882E+01	9.867E-01
12.45	2.214E+01	4.3	13.43	1.906E+01	8.236E-01
12.75	2.147E+01	4.4	13.76	1.849E+01	8.138E-01
12.95	2.097E+01	4.6	13.97	1.806E+01	8.230E-01
13.25	1.950E+01	6.3	14.30	1.680E+01	1.054E+00
13.45	1.813E+01	6.8	14.51	1.562E+01	1.059E+00
13.75	1.594E+01	9.4	14.83	1.374E+01	1.291E+00
13.95	1.334E+01	9.6	15.05	1.150E+01	1.106E+00
14.25	1.186E+01	12.6	15.37	1.022E+01	1.290E+00
14.45	8.887E+00	16.1	15.59	7.662E+00	1.231E+00
14.75	5.592E+00	16.1	15.91	4.822E+00	7.750E-01
14.95	4.672E+00	12.5	16.13	4.029E+00	5.040E-01
15.31	2.705E+00	19.0	16.51	2.333E+00	4.428E-01
15.80	1.113E+00	24.6	17.04	9.607E-01	2.366E-01
16.33	8.238E-01	30.0	17.61	7.112E-01	2.133E-01
16.75	1.446E+00	81.6	18.06	1.249E+00	1.019E+00
16.95	3.582E+00	18.7	18.28	3.094E+00	5.797E-01
17.25	4.268E+00	8.5	18.60	3.687E+00	3.141E-01
17.45	4.839E+00	12.3	18.82	4.181E+00	5.140E-01
17.75	6.005E+00	18.8	19.14	5.190E+00	9.750E-01
17.95	6.733E+00	11.5	19.36	5.820E+00	6.702E-01
18.25	7.327E+00	18.5	19.68	6.335E+00	1.173E+00
18.45	7.617E+00	6.2	19.89	6.587E+00	4.051E-01
18.75	7.840E+00	3.4	20.22	6.781E+00	2.331E-01
19.25	7.530E+00	6.9	20.75	6.516E+00	4.506E-01
19.75	4.657E+00	45.3	21.29	4.032E+00	1.826E+00
19.95	6.596E+00	14.2	21.51	5.711E+00	8.113E-01
20.45	5.362E+00	10.2	22.04	4.645E+00	4.716E-01
20.95	3.992E+00	13.6	22.58	3.460E+00	4.692E-01
21.34	2.811E+00	19.3	23.00	2.437E+00	4.710E-01
21.75	2.002E+00	17.0	23.44	1.736E+00	2.952E-01
22.34	1.219E+00	8.6	24.07	1.058E+00	9.083E-02
22.95	1.113E+00	11.3	24.73	9.664E-01	1.091E-01
23.25	1.471E+00	18.8	25.05	1.278E+00	2.405E-01
23.95	2.888E+00	5.3	25.80	2.511E+00	1.341E-01
24.75	3.060E+00	2.3	26.66	2.663E+00	6.085E-02
25.95	3.318E+00	3.4	27.95	2.891E+00	9.928E-02
26.25	2.990E+00	6.1	28.27	2.606E+00	1.599E-01
26.87	2.311E+00	13.3	28.93	2.016E+00	2.681E-01
27.25	1.276E+00	22.3	29.34	1.114E+00	2.482E-01
27.75	1.357E+00	7.8	29.87	1.185E+00	9.249E-02
28.45	1.013E+00	6.8	30.62	8.856E-01	5.982E-02
28.75	1.050E+00	4.5	30.94	9.178E-01	4.144E-02
29.34	1.017E+00	2.7	31.58	8.896E-01	2.369E-02
29.95	1.033E+00	2.9	32.23	9.051E-01	2.621E-02
30.25	1.037E+00	3.9	32.55	9.082E-01	3.521E-02
30.95	1.266E+00	3.8	33.30	1.110E+00	4.235E-02
31.45	1.340E+00	2.1	33.83	1.176E+00	2.436E-02
31.75	1.346E+00	2.2	34.15	1.182E+00	2.549E-02
32.45	1.359E+00	2.9	34.90	1.194E+00	3.454E-02
32.84	1.320E+00	4.6	35.31	1.161E+00	5.284E-02
33.25	1.097E+00	5.9	35.75	9.650E-01	5.727E-02
33.95	9.701E-01	5.2	36.50	8.544E-01	4.473E-02
34.45	8.714E-01	7.9	37.03	7.681E-01	6.059E-02
34.75	6.830E-01	8.8	37.35	6.023E-01	5.323E-02
35.25	6.332E-01	5.8	37.88	5.588E-01	3.253E-02
35.95	6.160E-01	4.0	38.63	5.442E-01	2.151E-02

36.34	6.250E-01	3.1	39.04	5.525E-01	1.714E-02
36.75	6.030E-01	3.3	39.48	5.334E-01	1.768E-02
37.45	6.717E-01	2.8	40.22	5.949E-01	1.695E-02
37.95	6.515E-01	3.2	40.76	5.775E-01	1.837E-02
38.25	6.950E-01	5.1	41.07	6.163E-01	3.126E-02
38.75	5.685E-01	4.6	41.61	5.046E-01	2.329E-02
39.45	5.937E-01	2.8	42.35	5.276E-01	1.465E-02
39.84	5.763E-01	4.6	42.76	5.125E-01	2.368E-02
40.25	4.743E-01	6.2	43.20	4.221E-01	2.606E-02
40.95	4.137E-01	3.6	43.94	3.686E-01	1.316E-02
41.45	3.995E-01	4.0	44.47	3.562E-01	1.442E-02
41.75	3.601E-01	4.4	44.79	3.213E-01	1.417E-02
42.25	3.727E-01	2.1	45.32	3.328E-01	6.824E-03
42.95	3.646E-01	4.8	46.06	3.260E-01	1.564E-02
43.34	3.468E-01	5.1	46.47	3.103E-01	1.590E-02
43.75	3.290E-01	2.9	46.90	2.946E-01	8.427E-03
44.45	3.667E-01	2.5	47.64	3.288E-01	8.247E-03
44.95	3.864E-01	3.9	48.17	3.468E-01	1.346E-02
45.25	3.533E-01	3.0	48.49	3.173E-01	9.425E-03
45.75	3.503E-01	2.6	49.02	3.149E-01	8.251E-03
46.45	3.895E-01	6.6	49.76	3.506E-01	2.308E-02
46.94	2.964E-01	10.8	50.17	2.670E-01	2.878E-02
47.25	3.596E-01	5.0	50.60	3.242E-01	1.630E-02
47.95	3.260E-01	5.0	51.34	2.943E-01	1.478E-02
48.45	2.618E-01	7.2	51.86	2.366E-01	1.699E-02
48.75	2.911E-01	6.2	52.18	2.632E-01	1.626E-02
49.25	2.365E-01	4.2	52.71	2.141E-01	9.017E-03
49.95	2.397E-01	2.3	53.44	2.164E-01	5.010E-03
50.80	2.442E-01	1.7	54.34	2.218E-01	3.800E-03
51.43	2.265E-01	2.7	55.00	2.060E-01	5.612E-03
51.84	2.312E-01	4.1	55.43	2.104E-01	8.621E-03
52.25	2.240E-01	2.6	55.86	2.041E-01	5.399E-03
52.45	2.311E-01	2.2	56.07	2.106E-01	4.559E-03
52.95	2.335E-01	3.8	56.59	2.130E-01	8.183E-03
53.45	2.248E-01	4.1	57.11	2.053E-01	8.366E-03
53.95	2.116E-01	2.2	57.64	1.935E-01	4.289E-03
54.45	2.125E-01	4.5	58.16	1.945E-01	8.750E-03
54.95	2.115E-01	5.0	58.68	1.938E-01	9.724E-03
55.45	1.812E-01	3.4	59.21	1.662E-01	5.658E-03
55.95	1.792E-01	4.4	59.73	1.646E-01	7.226E-03
56.40	1.873E-01	3.4	60.20	1.722E-01	5.826E-03
56.84	1.972E-01	4.2	60.66	1.815E-01	7.561E-03
57.34	1.805E-01	5.5	61.18	1.663E-01	9.193E-03
57.95	1.520E-01	5.4	61.82	1.402E-01	7.501E-03
58.45	1.355E-01	5.4	62.34	1.252E-01	6.698E-03
58.95	1.304E-01	7.5	62.86	1.206E-01	9.055E-03
59.45	1.295E-01	6.0	63.38	1.199E-01	7.242E-03
59.95	1.275E-01	4.7	63.90	1.182E-01	5.572E-03
60.45	1.253E-01	6.6	64.42	1.163E-01	7.662E-03
60.95	1.239E-01	4.7	64.94	1.151E-01	5.450E-03
61.45	1.280E-01	4.1	65.46	1.191E-01	4.873E-03
61.95	1.262E-01	5.4	65.98	1.175E-01	6.308E-03
63.34	1.149E-01	4.6	67.42	1.074E-01	4.889E-03
64.95	9.114E-02	5.5	69.08	8.552E-02	4.731E-03
66.45	5.861E-02	7.4	70.63	5.520E-02	4.078E-03
67.95	6.023E-02	5.6	72.18	5.694E-02	3.203E-03
69.34	5.634E-02	8.9	73.61	5.345E-02	4.735E-03
70.95	4.595E-02	9.6	75.26	4.378E-02	4.192E-03
72.45	2.790E-02	14.7	76.80	2.669E-02	3.921E-03
73.95	3.060E-02	11.2	78.33	2.938E-02	3.283E-03
75.34	2.744E-02	8.9	79.75	2.645E-02	2.355E-03
76.95	2.389E-02	8.9	81.39	2.313E-02	2.053E-03
78.45	1.730E-02	11.9	82.92	1.681E-02	2.000E-03
79.95	1.577E-02	10.9	84.44	1.539E-02	1.672E-03
81.34	1.062E-02	14.9	85.85	1.040E-02	1.553E-03
82.95	1.071E-02	13.5	87.47	1.054E-02	1.427E-03
84.45	6.884E-03	18.8	88.99	6.801E-03	1.276E-03
85.95	4.546E-03	21.5	90.50	4.510E-03	9.716E-04



SCATTERING OF 4-HE PARTICLES ON CR-52

ELAB = 104.000 MEV      Q = -4.580 MEV      I = 3 -  
 ECM = 91.979 MEV      K = 4.0443/FERMI      ETA = 1.51945

LABORATORY DATA			CM DATA		
THETA DEGREE	SIGMA MB/SR	DSIGMA %	THETA DEGREE	SIGMA MB/SR	DSIGMA MB/SR
10.34	1.364E+01	80.4	11.17	1.170E+01	9.414E+00
10.75	8.486E+00	397.4	11.61	7.283E+00	2.894E+01
10.95	7.096E+00	327.2	11.83	6.091E+00	1.993E+01
11.25	4.979E+00	78.3	12.15	4.274E+00	3.347E+00
11.45	5.324E+00	110.1	12.37	4.571E+00	5.033E+00
11.75	4.907E+00	55.4	12.69	4.213E+00	2.335E+00
11.95	3.567E+00	94.5	12.91	3.063E+00	2.894E+00
12.25	3.156E+00	243.8	13.23	2.711E+00	6.609E+00
12.45	2.888E+00	197.2	13.45	2.481E+00	4.892E+00
12.75	3.692E+00	59.7	13.77	3.172E+00	1.893E+00
12.95	4.204E+00	51.5	13.99	3.612E+00	1.859E+00
13.25	4.995E+00	42.2	14.31	4.293E+00	1.813E+00
13.45	5.498E+00	24.5	14.53	4.726E+00	1.160E+00
13.75	5.210E+00	8.1	14.85	4.479E+00	3.628E-01
13.95	5.010E+00	8.4	15.07	4.308E+00	3.618E-01
14.25	5.646E+00	6.9	15.39	4.855E+00	3.337E-01
14.45	5.831E+00	9.0	15.61	5.015E+00	4.518E-01
14.75	6.404E+00	4.8	15.93	5.509E+00	2.644E-01
14.95	6.384E+00	2.3	16.15	5.492E+00	1.281E-01
15.31	6.168E+00	1.8	16.53	5.309E+00	9.744E-02
15.79	6.227E+00	6.7	17.05	5.361E+00	3.609E-01
16.32	5.289E+00	24.4	17.63	4.556E+00	1.112E+00
16.75	5.213E+00	49.8	18.09	4.491E+00	2.238E+00
16.95	4.863E+00	28.5	18.30	4.190E+00	1.194E+00
17.45	3.686E+00	43.1	18.84	3.178E+00	1.369E+00
17.75	3.589E+00	106.2	19.16	3.094E+00	3.286E+00
17.95	3.096E+00	79.6	19.38	2.670E+00	2.124E+00
18.25	2.979E+00	85.6	19.70	2.570E+00	2.200E+00
18.75	2.512E+00	13.7	20.24	2.168E+00	2.975E-01
19.25	1.688E+00	18.6	20.78	1.458E+00	2.706E-01
19.75	1.795E+00	53.0	21.32	1.550E+00	8.212E-01
19.95	1.768E+00	7.9	21.53	1.527E+00	1.212E-01
20.45	1.982E+00	7.0	22.07	1.713E+00	1.202E-01
20.95	2.220E+00	5.0	22.61	1.920E+00	9.670E-02
21.34	2.398E+00	12.4	23.03	2.074E+00	2.577E-01
21.75	2.417E+00	19.5	23.47	2.092E+00	4.086E-01
22.34	2.513E+00	8.3	24.10	2.176E+00	1.807E-01
22.95	2.542E+00	4.2	24.76	2.202E+00	9.307E-02
23.25	2.132E+00	5.0	25.08	1.848E+00	9.146E-02
23.95	2.125E+00	3.7	25.83	1.844E+00	6.734E-02
24.75	1.453E+00	6.5	26.69	1.261E+00	8.249E-02
25.95	1.175E+00	7.8	27.98	1.022E+00	7.937E-02
26.25	1.092E+00	8.0	28.30	9.500E-01	7.648E-02
26.87	8.355E-01	30.8	28.97	7.272E-01	2.243E-01
27.25	9.066E-01	45.0	29.37	7.895E-01	3.549E-01
27.75	8.963E-01	21.1	29.91	7.811E-01	1.649E-01
28.45	1.089E+00	8.4	30.66	9.497E-01	7.956E-02
28.75	1.382E+00	5.3	30.98	1.206E+00	6.424E-02
29.34	1.380E+00	3.1	31.61	1.205E+00	3.686E-02
29.95	1.090E+00	4.4	32.26	9.528E-01	4.203E-02
30.25	1.058E+00	2.3	32.59	9.252E-01	2.152E-02
30.95	9.792E-01	4.4	33.33	8.570E-01	3.792E-02
31.45	7.657E-01	17.0	33.87	6.706E-01	1.138E-01
31.75	7.720E-01	19.4	34.19	6.763E-01	1.309E-01
32.45	7.373E-01	8.6	34.94	6.466E-01	5.566E-02
32.84	6.277E-01	10.0	35.35	5.508E-01	5.529E-02
33.25	8.638E-01	8.7	35.79	7.584E-01	6.615E-02
33.95	5.437E-01	9.5	36.54	4.779E-01	4.517E-02
34.45	6.615E-01	6.7	37.07	5.819E-01	3.918E-02
34.75	5.561E-01	9.4	37.39	4.894E-01	4.578E-02

35.25	7.343E-01	5.4	37.93	6.467E-01	3.511E-02
35.95	6.268E-01	4.5	38.67	5.527E-01	2.464E-02
36.34	5.791E-01	3.6	39.09	5.109E-01	1.863E-02
36.75	6.209E-01	4.1	39.52	5.482E-01	2.229E-02
37.45	4.962E-01	6.0	40.27	4.386E-01	2.642E-02
37.95	3.989E-01	5.6	40.80	3.529E-01	1.973E-02
38.25	3.758E-01	4.7	41.12	3.326E-01	1.577E-02
38.75	3.177E-01	4.9	41.65	2.814E-01	1.387E-02
39.45	2.842E-01	11.3	42.40	2.521E-01	2.838E-02
39.84	2.766E-01	17.5	42.81	2.455E-01	4.297E-02
40.25	2.388E-01	10.2	43.25	2.121E-01	2.164E-02
40.95	2.545E-01	8.6	43.99	2.264E-01	1.942E-02
41.45	2.540E-01	17.8	44.52	2.261E-01	4.030E-02
41.75	2.255E-01	18.2	44.84	2.008E-01	3.650E-02
42.25	2.428E-01	5.9	45.37	2.164E-01	1.284E-02
42.95	2.320E-01	11.0	46.11	2.071E-01	2.273E-02
43.34	2.750E-01	19.0	46.52	2.456E-01	4.678E-02
43.75	2.219E-01	12.6	46.96	1.983E-01	2.498E-02
44.45	2.120E-01	7.6	47.70	1.898E-01	1.448E-02
44.95	2.093E-01	19.8	48.23	1.875E-01	3.717E-02
45.25	2.008E-01	18.7	48.54	1.801E-01	3.365E-02
45.75	1.736E-01	8.4	49.07	1.558E-01	1.315E-02
46.45	1.886E-01	7.3	49.81	1.695E-01	1.239E-02
46.84	1.339E-01	12.9	50.22	1.204E-01	1.558E-02
47.25	1.740E-01	5.8	50.65	1.566E-01	9.050E-03
47.95	1.815E-01	5.8	51.39	1.636E-01	9.440E-03
48.45	1.282E-01	8.0	51.92	1.157E-01	9.208E-03
48.75	1.365E-01	4.4	52.24	1.233E-01	5.379E-03
49.25	1.311E-01	3.0	52.76	1.185E-01	3.608E-03
49.95	1.241E-01	4.0	53.50	1.123E-01	4.465E-03
50.80	1.153E-01	2.6	54.40	1.046E-01	2.769E-03
51.43	1.251E-01	4.4	55.05	1.136E-01	4.950E-03
51.84	1.399E-01	8.1	55.49	1.272E-01	1.031E-02
52.25	1.031E-01	10.4	55.92	9.380E-02	9.725E-03
52.45	1.139E-01	7.6	56.13	1.037E-01	7.829E-03
52.95	1.444E-01	7.2	56.65	1.316E-01	9.514E-03
53.45	1.188E-01	8.8	57.17	1.084E-01	9.583E-03
53.95	8.557E-02	8.6	57.70	7.813E-02	6.719E-03
54.45	9.942E-02	8.0	58.22	9.088E-02	7.313E-03
54.95	1.037E-01	8.0	58.75	9.490E-02	7.595E-03
55.45	8.495E-02	6.9	59.27	7.783E-02	5.333E-03
55.95	1.032E-01	6.5	59.79	9.466E-02	6.164E-03
56.40	1.066E-01	4.4	60.26	9.785E-02	4.275E-03
56.84	9.713E-02	7.6	60.72	8.928E-02	6.790E-03
57.34	1.255E-01	8.2	61.24	1.155E-01	9.415E-03
57.95	9.463E-02	8.5	61.88	8.720E-02	7.403E-03
58.45	1.128E-01	6.0	62.40	1.040E-01	6.192E-03
58.95	9.802E-02	8.8	62.92	9.054E-02	7.946E-03
59.45	6.858E-02	10.5	63.44	6.342E-02	6.670E-03
59.95	6.577E-02	8.3	63.96	6.090E-02	5.047E-03
60.45	5.605E-02	14.8	64.48	5.196E-02	7.713E-03
60.95	7.808E-02	7.4	65.00	7.247E-02	5.361E-03
61.45	7.741E-02	5.4	65.52	7.193E-02	3.880E-03
61.95	7.912E-02	6.9	66.04	7.361E-02	5.074E-03
63.34	7.468E-02	5.5	67.48	6.973E-02	3.830E-03
64.95	5.416E-02	6.8	69.15	5.077E-02	3.473E-03
66.45	3.668E-02	10.1	70.70	3.451E-02	3.472E-03
67.95	4.135E-02	7.3	72.25	3.906E-02	2.861E-03
69.34	4.865E-02	9.7	73.68	4.612E-02	4.483E-03
70.95	2.807E-02	13.0	75.33	2.673E-02	3.477E-03
72.45	1.991E-02	18.7	76.87	1.903E-02	3.554E-03
73.95	2.784E-02	11.8	78.40	2.671E-02	3.162E-03
75.34	3.165E-02	8.0	79.82	3.049E-02	2.448E-03
76.95	1.990E-02	10.1	81.46	1.925E-02	1.943E-03
78.45	1.414E-02	13.8	82.99	1.373E-02	1.898E-03
79.95	1.245E-02	11.8	84.51	1.215E-02	1.431E-03
81.34	1.098E-02	13.9	85.92	1.075E-02	1.494E-03
82.95	1.088E-02	12.9	87.55	1.070E-02	1.377E-03
84.45	8.495E-03	15.8	89.06	8.381E-03	1.328E-03
85.95	5.338E-03	20.1	90.57	5.296E-03	1.062E-03

SCATTERING OF 4-HE PARTICLES ON CR-52

FLAB = 104.000 MFV      Q = -2.370 MEV      I = 4 +  
 ECM = 94.189 MEV      K = 4.0926/FERMI      ETA = 1.50152

LABORATORY DATA			CM DATA		
THETA	SIGMA	DSIGMA	THETA	SIGMA	DSIGMA
DEGREE	MB/SR	%	DEGREE	MB/SR	MB/SR
9.34	4.393E+00	12.9	10.08	3.774E+00	4.855E-01
10.34	4.126E+00	8.2	11.16	3.546E+00	2.893E-01
10.75	4.487E+00	9.5	11.61	3.857E+00	3.650E-01
10.95	3.776E+00	12.3	11.82	3.246E+00	3.996E-01
11.25	3.973E+00	13.9	12.14	3.416E+00	4.737E-01
11.45	3.421E+00	12.6	12.36	2.942E+00	3.694E-01
11.75	3.202E+00	19.5	12.68	2.754E+00	5.383E-01
11.95	1.844E+00	39.3	12.90	1.586E+00	6.234E-01
12.25	2.484E+00	22.4	13.22	2.137E+00	4.777E-01
12.45	1.708E+00	28.7	13.44	1.470E+00	4.214E-01
12.75	1.530E+00	16.7	13.76	1.317E+00	2.200E-01
12.95	1.421E+00	15.7	13.98	1.223E+00	1.926E-01
13.25	1.424E+00	23.6	14.30	1.226E+00	2.899E-01
13.45	6.244E-01	64.8	14.52	5.376E-01	3.486E-01
13.75	3.722E-01	38.5	14.84	3.205E-01	1.171E-01
13.95	2.936E-01	51.2	15.06	2.529E-01	1.294E-01
14.25	2.413E-01	45.4	15.38	2.079E-01	9.435E-02
14.45	3.577E-01	36.9	15.59	3.082E-01	1.137E-01
14.75	4.603E-01	23.1	15.92	3.966E-01	9.149E-02
14.95	5.286E-01	17.9	16.13	4.556E-01	8.136E-02
15.33	6.588E-01	13.2	16.55	5.679E-01	7.507E-02
15.81	8.716E-01	11.4	17.06	7.516E-01	8.535E-02
16.33	9.248E-01	11.4	17.62	7.978E-01	9.063E-02
16.75	1.010E+00	109.9	18.07	8.712E-01	9.576E-01
16.95	1.249E+00	14.9	18.29	1.078E+00	1.610E-01
17.25	9.647E-01	34.8	18.61	8.328E-01	2.902E-01
17.45	7.747E-01	18.1	18.82	6.689E-01	1.209E-01
17.75	7.645E-01	43.2	19.15	6.603E-01	2.849E-01
17.95	9.465E-01	16.7	19.36	8.176E-01	1.365E-01
18.25	7.368E-01	115.0	19.69	6.366E-01	7.323E-01
18.45	7.230E-01	56.4	19.90	6.248E-01	3.525E-01
18.75	7.024E-01	13.7	20.22	6.071E-01	8.340E-02
19.25	3.939E-01	35.1	20.76	3.406E-01	1.194E-01
19.95	2.249E-01	22.2	21.51	1.946E-01	4.330E-02
20.45	1.730E-01	42.8	22.05	1.498E-01	6.414E-02
20.95	2.380E-01	35.3	22.59	2.061E-01	7.278E-02
21.34	2.886E-01	8.8	23.01	2.501E-01	2.208E-02
22.34	3.511E-01	9.6	24.08	3.045E-01	2.931E-02
22.95	3.712E-01	6.4	24.74	3.222E-01	2.057E-02
23.95	3.788E-01	8.5	25.81	3.291E-01	2.795E-02
25.95	1.938E-01	10.4	27.96	1.688E-01	1.754E-02
26.25	1.819E-01	13.3	28.28	1.585E-01	2.115E-02
26.87	1.310E-01	11.0	28.94	1.142E-01	1.252E-02
28.45	1.475E-01	7.8	30.63	1.288E-01	1.000E-02
29.34	1.676E-01	8.0	31.59	1.466E-01	1.170E-02
29.95	1.584E-01	10.1	32.24	1.386E-01	1.404E-02
30.25	1.537E-01	8.0	32.56	1.346E-01	1.079E-02
30.95	1.408E-01	9.4	33.31	1.234E-01	1.161E-02
31.45	1.242E-01	9.9	33.84	1.089E-01	1.074E-02
32.45	8.863E-02	18.7	34.91	7.784E-02	1.458E-02
32.84	7.476E-02	14.3	35.33	6.570E-02	9.399E-03
33.95	6.933E-02	16.7	36.51	6.103E-02	1.021E-02

34.45	7.917E-02	12.7	37.04	6.974E-02	8.831E-03
34.75	8.672E-02	10.2	37.36	7.643E-02	7.799E-03
35.95	8.461E-02	17.7	38.64	7.471E-02	1.319E-02
36.34	8.150E-02	10.6	39.06	7.201E-02	7.624E-03
37.45	7.261E-02	13.5	40.24	6.427E-02	8.692E-03
37.95	6.860E-02	13.2	40.77	6.077E-02	8.009E-03
38.25	5.905E-02	15.5	41.09	5.234E-02	8.136E-03
39.45	5.092E-02	17.9	42.36	4.522E-02	8.097E-03
39.84	4.075E-02	14.4	42.78	3.622E-02	5.228E-03
40.95	3.745E-02	18.8	43.95	3.335E-02	6.269E-03
41.45	3.842E-02	16.1	44.48	3.424E-02	5.502E-03
41.75	3.926E-02	13.7	44.80	3.501E-02	4.813E-03
42.95	4.129E-02	15.4	46.07	3.690E-02	5.686E-03
43.34	4.128E-02	14.1	46.49	3.692E-02	5.198E-03
43.75	4.069E-02	15.6	46.92	3.642E-02	5.677E-03
44.45	3.967E-02	14.2	47.66	3.555E-02	5.058E-03
44.95	4.073E-02	11.3	48.19	3.654E-02	4.131E-03
45.25	4.314E-02	12.0	48.51	3.872E-02	4.629E-03
46.45	3.636E-02	15.4	49.77	3.271E-02	5.024E-03
46.84	3.973E-02	8.5	50.18	3.577E-02	3.053E-03
47.25	3.722E-02	15.1	50.62	3.354E-02	5.069E-03
47.95	3.293E-02	14.2	51.35	2.972E-02	4.215E-03
48.45	3.517E-02	8.6	51.88	3.177E-02	2.728E-03
49.95	3.737E-02	9.2	53.46	3.386E-02	3.102E-03
50.81	3.689E-02	5.6	54.36	3.349E-02	1.886E-03
51.43	3.283E-02	8.5	55.01	2.984E-02	2.549E-03
51.84	3.234E-02	14.0	55.44	2.942E-02	4.110E-03
52.45	3.021E-02	6.8	56.08	2.752E-02	1.880E-03
52.95	2.909E-02	15.7	56.61	2.653E-02	4.171E-03
53.45	2.677E-02	15.5	57.13	2.444E-02	3.798E-03
53.95	2.521E-02	9.5	57.66	2.304E-02	2.195E-03
54.45	2.258E-02	23.8	58.18	2.066E-02	4.917E-03
54.95	2.278E-02	23.4	58.70	2.087E-02	4.875E-03
55.45	2.326E-02	8.1	59.23	2.133E-02	1.721E-03
55.95	2.636E-02	15.4	59.75	2.420E-02	3.718E-03
56.40	2.397E-02	12.1	60.22	2.203E-02	2.674E-03
56.84	2.236E-02	13.4	60.68	2.057E-02	2.765E-03
57.34	2.496E-02	16.9	61.20	2.290E-02	3.879E-03
57.95	2.506E-02	14.6	61.83	2.311E-02	3.382E-03
58.45	2.414E-02	14.2	62.36	2.229E-02	3.157E-03
58.95	1.828E-02	20.6	62.88	1.690E-02	3.479E-03
59.45	1.822E-02	22.0	63.40	1.686E-02	3.706E-03
59.95	1.581E-02	23.7	63.92	1.465E-02	3.466E-03
60.45	1.545E-02	32.7	64.44	1.433E-02	4.684E-03
60.95	1.815E-02	17.7	64.96	1.686E-02	2.988E-03
61.45	2.216E-02	13.2	65.48	2.061E-02	2.724E-03
61.95	2.015E-02	17.0	65.99	1.876E-02	3.180E-03
63.34	1.857E-02	14.4	67.44	1.735E-02	2.501E-03
64.95	1.279E-02	17.2	69.10	1.200E-02	2.060E-03
66.45	9.746E-03	26.0	70.65	9.176E-03	2.390E-03
67.95	9.006E-03	21.8	72.20	8.512E-03	1.856E-03
69.34	9.242E-03	33.3	73.63	7.818E-03	2.604E-03
70.95	7.784E-03	32.1	75.28	7.414E-03	2.383E-03
72.45	7.359E-03	36.0	76.82	7.037E-03	2.530E-03
73.95	6.933E-03	29.7	78.35	6.656E-03	1.980E-03
75.34	6.896E-03	21.3	79.77	6.636E-03	1.414E-03
76.95	4.450E-03	25.6	81.41	4.307E-03	1.104E-03
78.45	3.336E-03	39.1	82.94	3.242E-03	1.266E-03
79.95	2.095E-03	41.4	84.46	2.044E-03	8.461E-04
81.34	1.786E-03	47.3	85.87	1.749E-03	8.281E-04
82.95	1.551E-03	57.7	87.50	1.526E-03	8.805E-04
84.45	1.331E-03	53.8	89.01	1.315E-03	7.071E-04
85.95	1.054E-03	58.3	90.52	1.046E-03	6.096E-04